HHS Public Access

Author manuscript

Chem Rev. Author manuscript; available in PMC 2017 July 13.

Published in final edited form as:

Chem Rev. 2016 July 13; 116(13): 7501–7528. doi:10.1021/acs.chemrev.5b00644.

Modeling Molecular Interactions in Water: From Pairwise to Many-Body Potential Energy Functions

Gerardo Andrés Cisneros[†], **Kjartan Thor Wikfeldt**[‡], **Lars Ojamäe**[#], **Jibao Lu**[||], **Yao Xu**[⊥], **Hedieh Torabifard**[†], **Albert P. Bartók**[@], **Gábor Csányi**[@], **Valeria Molinero**[||], and **Francesco Paesani**[*,▽]

[†]Department of Chemistry, Wayne State University, Detroit, Michigan 48202, United States [‡]Science Institute, University of Iceland, VR-III, 107, Reykjavik, Iceland [§]Department of Physics, Albanova, Stockholm University, S-106 91 Stockholm, Sweden [||]Department of Chemistry, The University of Utah, Salt Lake City, Utah 84112-0850, United States [⊥]Lehrstuhl Physikalische Chemie II, Ruhr-Universität Bochum, 44801 Bochum, Germany [@]Engineering Laboratory, University of Cambridge, Trumpington Street, Cambridge CB21PZ, United Kingdom [#]Department of Chemistry, Linköping University, SE-581 83 Linköping, Sweden [▽]Department of Chemistry and Biochemistry, University of California San Diego, La Jolla, California 92093, United States

Abstract

Almost 50 years have passed from the first computer simulations of water, and a large number of molecular models have been proposed since then to elucidate the unique behavior of water across different phases. In this article, we review the recent progress in the development of analytical potential energy functions that aim at correctly representing many-body effects. Starting from the many-body expansion of the interaction energy, specific focus is on different classes of potential energy functions built upon a hierarchy of approximations and on their ability to accurately reproduce reference data obtained from state-of-the-art electronic structure calculations and experimental measurements. We show that most recent potential energy functions, which include explicit short-range representations of two-body and three-body effects along with a physically correct description of many-body effects at all distances, predict the properties of water from the gas to the condensed phase with unprecedented accuracy, thus opening the door to the long-sought "universal model" capable of describing the behavior of water under different conditions and in different environments.

Graphical abstract

[*]Corresponding Author: fpaesani@ucsd.edu.

Notes

The authors declare no competing financial interest.

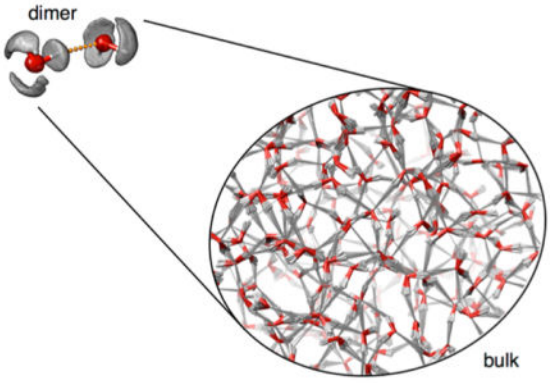

1. INTRODUCTION

Computer simulations have become an indispensable tool for characterizing the properties of water at the molecular level, often providing fundamental insights that are otherwise difficult to obtain by other means. However, both the realism and the predicting power of a computer simulation directly depend on the accuracy with which the molecular interactions and the overall system dynamics are described. Rigorously, realistic computer simulations of water should include an accurate representation of the underlying Born–Oppenheimer potential energy surface (PES) in combination with a proper treatment of the nuclear motion at a quantum-mechanical level.[1–3] Along these lines, different theoretical and computational approaches have been proposed, which can be conveniently separated in two main groups depending on how the water PES is described. The first group includes simulation approaches that use a set of predefined analytical functions to represent the underlying PES of the water system of interest as a function of the corresponding molecular coordinates. These analytical potential energy functions are historically referred to as “force fields”.[4–8] The second group includes the so-called “ab initio” approaches in which the water PES is obtained “on the fly” by performing quantum-chemical calculations to solve the electronic time-independent Schrödinger equation for a given molecular configuration.[9–14] Ab initio approaches can be further distinguished in methods based on wave function theory (WFT) and density functional theory (DFT). Independent of how the water PES is represented, the nuclear dynamics can then be described at the classical level using Newton’s equations of motion or at the quantum-mechanical level by solving the corresponding nuclear time-dependent Schrödinger equation using grid methods, wave packets, semiclassical approaches, and methods built upon Feynman’s path-integral formalism.[15–21]

As part of this thematic issue “Water - The Most Anomalous Liquid”, this article reviews recent progress in the development and application of analytical potential energy functions (PEFs) that aim at correctly representing many-body effects in water from the gas to the liquid phase. Specific focus is on different classes of PEFs built upon a hierarchy of approximate representations of many-body effects and on their ability to accurately reproduce reference data obtained from state-of-the-art (i.e., correlated) electronic structure calculations. With this objective in mind, we introduce and describe the many-body expansion (MBE) of the interaction energy in section 2. Purely pairwise PEFs are only

briefly mentioned in section 3, while different classes of many-body PEFs are described in section 4. Within each class, the accuracy of the individual PEFs is assessed systematically through the analysis of the energetics of water clusters for which correlated electronic structure calculations are possible. To determine how the accuracy of each PEF in representing the fundamental interactions between water molecules translates into the ability of the same PEF to reproduce measurable quantities, comparisons with experimental data for representative structural, thermodynamic, and dynamical properties of liquid water are also discussed. Although the ability to correctly reproduce the experimental data is the ultimate goal of a computer simulation, "getting the right results for the right reasons" is even more important for the correct interpretation of the underlying molecular mechanisms. We will show that the apparent perfect agreement with the results of experimental measurements that are mainly sensitive to the average molecular behavior is often the result of error cancellation between different many-body contributions to the total interaction energy. These deviations from the actual Born–Oppenheimer PES effectively preclude a rigorous and quantitative interpretation of the experimental measurements, which has led, in the past, to the proliferation of water models. As discussed in section 4, the advent of explicit many-body PEFs holds great promise for a physically correct, molecular-level description of the properties of water across different phases. Building upon recent achievements and, in several cases, unprecedented accuracy of many-body PEFs, future development and applications to aqueous systems are presented in section 5.

2. MANY-BODY EXPANSION OF THE INTERACTION ENERGY

The global PES of a system containing N interacting water molecules can be formally expressed in terms of the many-body expansion of the interaction energy as a sum over n-body terms with $1 \le n \le N$,[22]

$$V_N(\mathrm{r}_1, \ldots, \mathrm{r}_N) = \sum_{i=1}^{N} V_{1\mathrm{B}}(\mathrm{r}_i) + \sum_{i<j}^{N} V_{2\mathrm{B}}(\mathrm{r}_i, \mathrm{r}_j) + \sum_{i<j<k}^{N} V_{3\mathrm{B}}(\mathrm{r}_i, \mathrm{r}_j, \mathrm{r}_k) + \ldots + V_{N\mathrm{B}}(\mathrm{r}_1, \mathrm{r}_2, \mathrm{r}_3, \ldots, \mathrm{r}_N) \quad (1)$$

where r_i collectively denotes the coordinates of all atoms of the ith water molecule. In eq 1, $V_{1\mathrm{B}}$ is the one-body (1B) potential that describes the energy required to deform an individual molecule from its equilibrium geometry. All higher n-body (nB) interactions, $\mathrm{V}_{n\mathrm{B}}$, are defined recursively through

$$V_{n\mathrm{B}}(\mathrm{r}_1, \ldots, \mathrm{r}_n) = V_n(\mathrm{r}_1, \ldots, \mathrm{r}_n) - \sum_{i=1}^{N} V_{1\mathrm{B}}(\mathrm{r}_i) - \sum_{i<j}^{N} V_{2\mathrm{B}}(\mathrm{r}_i, \mathrm{r}_j) - \ldots - \sum_{i<j<\ldots<n-1}^{N} V_{(n-1)\mathrm{B}}(\mathrm{r}_i, \mathrm{r}_j, \mathrm{r}_k) \quad (2)$$

The PEFs developed for computer simulations of water can be conveniently classified according to the level of approximation used to represent the different terms of eq 1. Starting with the 1B term, most common, and least realistic, force fields assume rigid geometries for the water molecules, with intramolecular flexibility being explicitly taken into account only in more sophisticated energy expressions. The different treatment of the $V_{1\mathrm{B}}$ term thus leads to a separation of the existing PEFs in two main groups, the “rigid-monomer” and the “flexible-monomer” PEFs. Within each group, analytical PESs for water can be further distinguished based on how all $V_{n\mathrm{B}}$ terms of eq 1, with $n > 1$, are described.

Most common force fields only include up to the two-body (2B) term and assume that the sum of pairwise additive contributions provide a sufficiently accurate representation of the actual multidimensional Born–Oppenheimer PES. In the so-called “effective” pair potential energy functions, all three-body (3B) and higher-body contributions are merged into an effective 2B term. Analytical PEFs that are obtained by fitting to experimental data, commonly referred to as “empirical” force fields, are most often of this type. Experimental data may also be combined with results from quantum chemical calculations to fit empirical force fields. Alternatively, analytical PEFs can be systematically derived by fitting to electronic structure data for water dimers, trimers, etc. In this case, the application of eq 1 leads to ab initio representations of the multidimensional Born–Oppenheimer PES. If the fit is carried out only on dimer energies, the many-body expansion of the total interaction energy is truncated at the 2B level, resulting in a strictly pairwise additive representation of the PES. In most analytical PEFs that go beyond the pairwise approximation, higher-order terms are collectively represented through classical many-body polarization.

More recently, *ab initio* PEFs including explicit 3B terms have also been developed. For water in the condensed phase, many-body interactions are responsible for nontrivial effects, which may either lower (cooperative effects) or increase (anticooperative effects) the total interaction energy relative to the sum of all pairwise contributions. Several systematic studies of the interaction energy for small clusters carried out using electronic structure methods shows that eq 1 converges rapidly for water. However, nonadditive effects are generally nonnegligible,[22–31] with 3B contributions being as large as ~15–20% of the total interaction energy for cyclic structures. Four-body (4B) effects are responsible, on average, for ~1% of the total interaction energy.[23,29–31] Taking advantage of the rapid convergence of eq 1, a novel computational scheme, called “stratified approximation many-body approach” or SAMBA, has recently been shown to provide highly accurate interaction energies for water clusters through the application of progressively lower-level electronic structure methods to subsequent terms of the MBE.[31]

Besides representing a rigorous approach to the development of analytical PEFs for molecular systems ranging from the gas-phase dimer to small clusters and the liquid phase, the MBE in eq 1 also provides a quantitative way to assess the ability of existing models in describing the water interactions. In this context, Figures 1 and 2, which are derived from the analysis originally reported in ref 32, show correlation plots between 2B and 3B reference interaction energies with the corresponding values calculated using several empirical nonpolarizable (blue) and polarizable (light blue) force fields, semiempirical methods (green), DFT models (yellow), explicit many-body PEFs (orange), and second-order Møller–Plesset (MP2) theory (red). The reference energies were calculated at the coupled cluster level including single, double, and perturbative triple excitations [i.e., CCSD(T)] with the aug-cc-pVTZ basis set[33,34] and corrected for the basis set superposition error (BSSE) using the counterpoise method.[35]

Since, by construction, the 2B term of the empirical pairwise additive PESs (i.e., aSPC/Fw[36] and q-TIP4/F[37]) tries to effectively compensate for the neglect of higher-order contributions, large deviations from the reference CCSD(T)/aug-cc-pVTZ values are found over the entire range of interaction energies considered in Figure 1. The explicit inclusion of 3B contributions (e.g., E3B2[38]) and polarization effects (e.g., AMOEBA2003,[39] TTM3-F,[40] and TTM4-F[41]) clearly improves the agreement with the reference data at the 2B level and provides a more physically realistic description of higher-body effects. The comparison with the CCSD(T)/aug-cc-pVTZ data also indicates that the overall accuracy of the different polarizable models considered in this analysis is particularly sensitive to the specific functional form used to represent induction effects (see section 4.2).

Semiempirical models (e.g., PM3,[42] PM6,[43] and SCP-NDDO[44,45]) display similar accuracy as polarizable force fields, with the SCP-NDDO model, which includes an additional term describing induction interactions, providing the closest agreement with the reference data. In general, DFT models, including GGA without (e.g., BLYP[46,47] and PBE[48]) and with (e.g., BLYP-D[49]) dispersion corrections, hybrid (e.g., B3LYP[50] and PBE0[51]), and nonlocal functionals (e.g., VV10[52]), predict 2B and 3B interaction energies in reasonably good agreement with the CCSD(T)/aug-cc-pVTZ values. Appreciable differences, however, can be found at the 2B level, which vary significantly depending on how exchange, correlation, and dispersion contributions are treated within each functional. The current status of DFT models for water is reviewed in a separate article as part of this thematic issue.[53] Figures 1 and 2 also show that high accuracy, often more superior than that associated with DFT models and comparable to that obtained at the MP2 level of theory, can be achieved by analytical many-body PEFs (e.g., WHBB[54] and HBB2-pol[55]) that explicitly include 2B and 3B contributions derived from multidimensional fits to correlated electronic structure data and describe higher-order effects through (classical) many-body induction.

In the following sections, all different classes of many-body PEFs for water, which are built upon different levels of approximations to eq 1, are reviewed systematically in terms of their ability to accurately reproduce reference data obtained from both state-of-the-art electronic structure calculations and experimental measurements. The objective of this review article is to provide the reader with a comprehensive overview of modern PEFs that aim at modeling the molecular properties of water through a physically correct representation of many-body

effects. Due to space constraints and considering that many of the PEFs described in this review are still under development, only a limited number of direct comparisons between different PEFs is presented. These comparisons, along with tables summarizing the "performance" of different PEFs in reproducing experimental data, are used to assess both merits and shortcomings of different theoretical and computational approaches to model many-body effects in water. The reader is referred to other articles of this thematic issue for specific applications of computer simulations to the study of structural, thermodynamic, and dynamical properties of water under different conditions and in different environments.

3. PAIRWISE ADDITIVE ANALYTICAL POTENTIAL ENERGY FUNCTIONS

To date, pairwise additive PEFs, like the aSPC/Fw[36] and q-TIP4P/F[37] models of Figures 1 and 2, are the most common representations of the interactions between water molecules used in conventional computer simulations. By construction, these PEFs do not include an explicit treatment of many-body effects but approximate the total interaction energy through an effective 2B term that is empirically parametrized to reproduce experimental data. In addition, the vast majority of these PEFs, including the popular TIPnP[56–58] and SPC∗[59,60] families among many others, assume the water molecules to be rigid. Since this class of PEFs has recently been reviewed, it will not be further discussed here, and we direct the interested reader to refs 61 and 62 for specific details.

Building upon rigid-monomer parametrizations, intramolecu-lar flexibility has also been added empirically to some of the most popular pairwise additive PEFs, which have then been employed in both classical and quantum molecular simulations.[36,37,63–70] Although the overall performance of flexible force fields (e.g., the aSPC/Fw[36] and q-TIP4P/F[37] models) is comparable to that of the original rigid models, the inclusion of intramolecular flexibility enables a more direct assessment of nuclear quantum effects in determining both thermodynamic and dynamical properties.[37,66,69] The interested reader is directed to the review article in this thematic issue devoted specifically to the analysis of nuclear quantum effects in water.[71]

A different class of pairwise potentials can be derived from eq 1 relying only on ab initio data for the water dimers but still assuming rigid monomers. The first such potential, MCY, was developed by Matsuoka et al.[72] The MCY potential was parametrized by fitting two analytical functions to reproduce the energetics of 66 water dimer structures calculated at the configuration interaction level including single excitations (CIS). The original MCY potential was subsequently used as a starting point for further improvements which led to the development of a new version of the potential with flexible monomers,[73] a refinement of the parameters based on the analysis of the vibrational frequencies,[74–76] and other more general reparame-terizations.[77] Several strictly pairwise PEFs, derived entirely from ab initio data, were proposed in the 1990s,[78,79] which served as a starting point for subsequent developments of rigorous many-body representations of the interaction energies (see section 4.3).

The MCY functional form was employed by Mas et al. to parametrize an analytical PEF for water using symmetry adapted perturbation theory (SAPT) calculations performed on over

1000 water dimers with rigid monomers.[80,81] Within the SAPT formalism, individual contributions to noncovalent interactions between two molecules can be directly determined through perturbation theory, avoiding separate calculations of monomer and dimer energies.[82] Although SAPT provides a systematic decomposition of the total interaction energy into physically based components (e.g., electrostatics, exchange, induction, and dispersion), the water model developed by Mas et al. was directly obtained from a linear least-squares fit of the total energy to the MCY functional form.[80,81] The agreement between the calculated and measured second virial coefficient demonstrated the overall accuracy of the SAPT-derived PEF, which effectively represents the first attempt at using large sets of high-level ab initio data to construct an accurate representation of the 2B term of the MBE for water shown in eq 1.

When employed in computer simulations, both empirical and ab initio pairwise PEFs have been successful at reproducing at least some of the water properties, providing fundamental insights at the molecular level. However, by construction, pairwise representations of the total interaction energy suffer from intrinsic shortcomings that limit their transferability to more complex aqueous solutions and heterogeneous environments. These shortcomings are primarily associated with the specific functional form adopted by pairwise PEFs which, including only up to 2B contributions, neglect all many-body effects (see Figure 2).[83] Therefore, the logical next step in the accurate representations of the interactions between water molecules requires the development of analytical PEFs that include either implicitly or explicitly nonadditive effects arising from many-body interactions.

4. MANY-BODY ANALYTICAL POTENTIAL ENERGY FUNCTIONS

4.1. Implicit Many-Body Potential Energy Functions: Empirical Models

Several theoretical analyses based on electronic structure data have demonstrated that many-body interactions contribute, on average, ~ 20% to the total interaction energy of water clusters, with 3B contributions representing up to ~18%.[22–30,84–86] As discussed in section 3, in pairwise PEFs such as those employed in the popular TIPnP[56–58] and SPC*[59,60] force fields, many-body contributions are only represented in an effective way in a mean-field fashion.[87] This appears to be a reasonable approximation for a qualitative modeling of homogeneous aqueous systems like bulk water as shown by the success of some pairwise force fields in reproducing several structural, thermodynamic, and dynamical properties of liquid water.[61,62] Although it was shown that many-body effects can be decomposed, at least to some extent, into effective pairwise contributions using force-matching,[88] more recent studies have demonstrated that the explicit account of 3B effects is essential for a physically correct description of heterogeneous environments such as the air/water interface.[89,90]

3B Interactions have also been shown to play an important role in coarse-grained (CG) representations of the actual multidimensional Born–Oppenheimer PESs.[91–101] By construction, many-body effects in CG models can hardly be accounted for by using only pairwise potential energy functions. For example, Johnson et al. derived coarse-grained effective pair potentials from simulations with TIP4P-Ew rigid and nonpolarizable model[58] and demonstrated that pairwise CG models can reproduce some waterlike anomalies but are unable to simultaneously reproduce structural and thermodynamic properties.[102] A more

quantitative representation of many-body effects in CG models of water can be achieved by adding an empirical 3B term to the pairwise expression of the interaction energy.[100,103] An example of CG representations including 3B effects is the mW model,[100] which adopts the same 2B and 3B energy expressions as the Stillinger-Weber model for silicon,[104] and was parametrized to reproduce the experimental melting temperature, enthalpy of vaporization, and density of liquid water at ambient conditions. The mW model qualitatively reproduces the structure (Figure 3a) and the temperature dependence of several thermodynamic properties of liquid water, including the density maximum at ambient pressure although the actual location is shifted to a slightly lower temperature relative to the experimental value (Figure 3b). It was also shown that mW is more accurate than some atomistic models (e.g., SPC/E, TIP3P, and TIP4P) in representing several thermodynamic properties, including the melting temperature of ice I_h, the liquid density at the melting point, the enthalpy of melting, and the surface tension.[100,105]

Explicit 3B terms have also been introduced in atomistic force fields. For example, the E3B models utilize the TIP4P and TIP4*P*/2005 force fields as baseline PEFs to which an explicit three-body term is added to recover cooperative and anticooperative effects associated with different hydrogen-bonding arrangements.[38,106,107] Additional 2B terms are also added to the original pairwise expressions to remove spurious 3B contributions. The E3B2 model was parametrized to reproduce six experimental properties (diffusion constant, rotational correlation time, liquid density, surface tension, melting point, and ice I_h density).[38] The addition of an explicit 3B term was shown to improve the accuracy with which the properties of water in heterogeneous environments, including water clusters and the air/water interface, could be calculated.[38,89,106] The E3B2 model correctly reproduces several properties of the liquid phase, although the calculated oxygen–oxygen radial distribution function shown in Figure 3a appears to be too structured compared to the most recent results derived from neutron-diffraction measurements.[108] The static dielectric constant and low-frequency infrared spectra calculated with the E3B2 model for both liquid water and ice I_h are also in good agreement with the corresponding experimental data over wide temperature ranges, although one distinct fitting parameter is required for each phase.[109] A new parametrization of the E3B model (E3B3) has recently been introduced.[107] E3B3 is built upon the TIP4*P*/2005 force field and shows higher accuracy than the original E3B2 model, especially in reproducing the temperature dependence of structural and thermodynamic properties (e.g., the liquid density shown in Figure 3b). Although the E3B models represent an improvement over common pairwise additive force fields, a recent analysis of the heterodyne-detected vibrational sum-frequency generation (HD-vSFG) spectrum of the air/water interface in terms of many-body contributions suggests that, due to the empirical parametrization, 3B effects are possibly overemphasized in the E3B models.[90]

4.2. Implicit Many-Body Potential Energy Functions: Polarizable Models

Alternatively to empirical parametrizations, it is possible to develop PEFs that take into account many-body contributions derived from a systematic decomposition of the intermolecular interactions based on quantum-chemical calculations. Several energy decomposition analysis (EDA) methods have been developed over the years. These methods can be classified as variational such as the Kitaura-Morokuma and similar schemes[110–120] or

perturbational.[121–126] In most cases, these methods decompose the intermolecular interaction energies into several terms including Coulomb, exchange-repulsion, dispersion, polarization, charge-transfer, and possibly higher-order terms. The last four terms effectively encompass many-body contributions to the interaction energy.

The most common approach to including many-body effects in analytical PEFs is through the addition of a polarization (or induction) term to the energy expression. As for the pairwise PEFs described in section 3, polarizable force fields can be classified as empirical or ab initio, depending on how the parametrization is performed. A list of popular polarizable models, including specific details about the induction scheme adopted in the energy expression and type of data used in the parametrization, is reported in Table 1. One of the earliest attempts to account explicitly for polarization effects in the interactions between water molecules is represented by the model constructed by Stillinger and David which was applied to small clusters and ion monohydrates.[127] Besides including isotropic dipole polarizability on the oxygen atom of each water molecule, the model was based on charged ions and a dissociable form of the intramolecular potential energy. Another early simulation study of polarization effects in liquid water was performed by Barnes et al. using the polarizable electrupole (PE) model.[83] The PE model describes each water molecule as a single site carrying both the experimental static dipole and quadrupole moments along with an isotropic dipole polarizability. This specific functional form was derived from the results of electronic structure calculations indicating the presence of 20–30% stronger hydrogen bonds in trimers and tetramers than in the dimer as well as a strong increase of the molecular dipole moment in going from the gas phase to bulk ice I_h. Although the PE model did not display high accuracy, it inspired subsequent developments of polarizable force fields. Indeed, representing many-body effects through polarizable dipoles has become standard practice.

On the basis of the early studies by Stillinger and David[127] and Barnes et al.,[83] several empirical polarizable force fields have been developed, including the model by Lybrand and Kollman,[128] the POL3 model,[129] the SCP-pol and TIP4P-pol models,[130] the TIP4P-based polarizable model parametrized with neural networks,[131] the five-site model by Stern et al.,[132] as well as ab initio polarizable force fields such as OSS.[133] As discussed by Guillot,[61] however, the history of force field developments has shown that simply adding dipole polarizability to existing point-charge models does not lead to the general improvement in accuracy and/or transferability that might be expected. A likely reason for this is that the electric field generated by point-charge water models is too inaccurate for realistic dipole induction calculations.

Alternatively to point dipoles, polarization contributions have also been included in water force fields through the charge-on-spring (also known as Drude oscillator) scheme. In the most common implementations, an additional partial charge is connected by a harmonic spring to one of the sites (usually the oxygen atom or the site carrying the negative charge) that are used to define the electrostatic properties (e.g., dipole and quadrupole moments) of an isolated water molecule. Examples of charge-on-spring water models are the SWM4-DP,[134] SWM4-NDP,[135] SWM6,[136] COS,[137–139] and BK3[140] models. Since these polarizable force fields assume rigid-monomer geometries and thus neglect 1B contributions to the

interaction energy, they will not be discussed further here. The interested reader is directed to the original studies for specific details.

An example of an analytical PEF that was derived using both experimental and ab initio data is the AMOEBA model.[39,141,142] New versions of AMOEBA, termed inexpensive AMOEBA (iAMOEBA) and AMOEBA14, have recently been proposed.[143] iAMOEBA only includes contributions to the polarization term from the permanent fields and the remaining parameters have been optimized to reproduce both ab initio and selected experimental data. Although the iAMOEBA model improves the description of water clusters and liquid water compared to the original AMOEBA model, non-negligible deviations from highly correlated electronic structure reference data were found at the 3B level.[144] Torabifard et al. have recently reported an AMOEBA water model based on a different set of distributed multipoles obtained from GEM.[145] Several properties have been calculated across a range of temperatures and compared to the experimental counterparts. This new AMOEBA model shows very good agreement for density, heat of vaporization, and diffusion coefficients over the tested temperature range.[146] Other polarizable water models that rely on the use of diffuse functions (e.g., single spherical Gaussians) instead of point charges or multipoles have also been proposed.[147,148]

One of the first ab initio water PEFs taking explicitly induced multipolar polarizabilities into account was developed by Campbell and Mezei.[149] This PEF was fitted to the energies of 229 water dimers calculated at the HF level. Several other potential energy functions have been proposed, which make only use of ab initio data in the fitting process. These PESs include the models by Yoon et al.[25] and Li et al.,[150] the NEMO model by Karlstrom and co-workers,[151–157] the X-pol model by Gao and co-workers,[158–161] the multipolar model of Popelier and coworkers based on quantum chemical topology,[162–165] and the model by Torheyden and Jansen.[166]

Other PESs derived from ab initio data include additional many-body terms to improve the description of the intermolecular interactions between water molecules. One of the first examples that attempted to reproduce every component of the Kitaura-Morokuma decomposition is the Singh-Kollman model.[167] The effective fragment potential (EFP) also includes terms such as charge transfer to account for many-body effects.[168–172] Similar analytical PEFs have recently been proposed.[173] SIBFA is an example of a force field based on the individual reproduction of each term of the ab initio energy decomposition analysis.[174–177] The SIBFA functional form uses damped distributed point multipoles for the calculation of the intermolecular Coulomb interactions as well as the electrostatic potential and electric field necessary for the calculation of the second order (polarization and charge-transfer) terms.

The Gaussian electrostatic model (GEM) follows the same philosophy as SIBFA in systematically reproducing each EDA term.[178–185] However, GEM uses explicit molecular electronic density for each fragment instead of a discrete distribution. The use of explicit densities results in a more accurate description of the intermolecular interaction, especially at medium to short range, since the penetration errors are virtually eliminated.[145] Recently, a new water PEF based on GEM and AMOEBA, called GEM*, has been developed. GEM*

combines the Coulomb and exchange-repulsion terms from GEM with the polarization, bonded and (modified) dispersion terms from AMOEBA. GEM* was fitted exclusively to ab initio data from water dimers and trimers and reproduces both binding energies of water clusters[186–188] and bulk properties such as the heat of vaporization.[189] In the first implementation of GEM*, all quantum data was obtained at the MP2/aug-cc-pVTZ level (including the reference molecular density) for comparison with the reference AMOEBA03 potential. In general, the calculation of the exchange contribution in some of the above-mentioned force fields, such as GEM and SIBFA, is performed in a pairwise manner. However, many-body effects from exchange interactions also arise from higher-order terms (e.g., polarization, charge transfer, and dispersion). These effects can be included explicitly through, for example, the use of the Axilrod–Teller triple dipole function employed by Li et al.[150] and the triple overlap function as included in SIBFA.[190] Recent efforts have focused on ways to improve the efficiency for the evaluation of the integrals required by GEM* (and GEM) as well as on more accurate fits performed using reference data from both higher-level electronic structure calculations and MB-pol dimer and trimer potential energy surfaces.[144,191]

In the 2000s, Xantheas and co-workers introduced the TTM (Thole-type model) potential energy functions[192–196] that, for the first time, made use of a highly accurate 1B term derived from high-level ab initio calculations by Partridge and Schwenke.[197] The latest versions of the TTM models (TTM3-F[40] and TTM4-F[41]) employ point dipoles with Thole-type damping[198] between the charges and the induced dipoles and between the induced dipoles themselves. As shown in Figures 1 and 2, while both TTM3-F and TTM4-F PEFs deviate significantly from the CCSD(T) reference data at the 2B level, TTM4-F effectively reproduces 3B effects with the same accuracy as MP2, reinforcing the notion that high-order interactions in water can be effectively represented through classical many-body polarization. The TTM PEFs were shown to reproduce the properties of water clusters, liquid water, and ice reasonably well.[199–202] Since the 1B term of the TTM PEFs correctly describes intramolecular charge transfer, both TTM3-F and TTM4-F reproduce the observed increase of the HOH angle going from the gas to the condensed phase and the correct IR spectrum of the HOH bend. However, some inaccuracies were identified in modeling the OH stretching vibrations, with both TTM3-F and TTM4-F predicting an absorption line shape that is red-shifted compared to the experiment.[203–205] In addition, as shown in Figure 4, the apparent agreement with reference data achieved by the TTM3-F model is often the result of fortuitous error cancellation between different terms of the MBE. Closely related to the TTM family are the DDP2,[206] POLIR,[207] and POLI2VS[208] polarizable force fields, with the last two models being specifically developed to simulate the infrared spectrum of liquid water. Direct comparisons between AMOEBA14, TTM3-F, TTM4-F, PO-LI2VS, and GEM* are shown in Figure 4.

Following a different approach based on intermolecular perturbation theory, an important early attempt to reach higher accuracy in modeling water clusters, at the expense of computational efficiency, was made by Stone and co-workers through the development of the anisotropic site potential (ASP-W).[209] The ASP-W model, as the subsequent improved versions ASP-W2 and ASP-W4,[210] is based on a distributed multipole expansion of the electric field around the water molecule, with the expansion going from point charges

(monopoles) up to the quadrupole on the oxygen atom and dipole on the hydrogen atoms. Induction effects are treated by dipole as well as quadrupole polarizabilities, and the dispersion and short-range exchange-repulsion energy components are treated by detailed anisotropic functions fitted to ab initio data. Despite their elaborate construction, the ASP-W models were shown to contain inaccuracies in the description of water clusters, while simulations of liquid water have not yet been attempted. Building on the studies by Stone and co-workers, Goldman et al. took advantage of accurate experimental measurements of vibration–rotation tunneling (VRT) spectra of the water dimer and performed several reparametrization of the original ASP-W model to match the experimental tunneling splittings.[211] The latest version, called VRT(ASP-W)III, describes the dimer potential energy surface with spectroscopic accuracy, albeit with fixed intramolecular geometry. When applied to Monte Carlo simulations of liquid water, VRT(ASP-W)III predicted a too weakly structured liquid compared to experimental diffraction data, even without the inclusion of nuclear quantum effects.[212]

The recently proposed single-center multipole expansion (SCME) model[213] follows a similar philosophy as the ASP models but includes an important simplification which renders it more computationally efficient as well as physically transparent. From the analysis of electric fields in ice and around water clusters, Batista et al.[214,215] observed that an electric induction model based on a multipole expansion around a single site (the molecular center of mass) agree well with DFT and MP2 calculations when the expansion is carried out up to and including the hexadecupole moment, with induction effects treated by dipole and quadrupole polarizabilities. The importance of including the hexadecupole moment in the electrostatics of ice was also highlighted in the work of Tribello and Slater,[216] who showed that effective force fields consistently fail to describe the energetics of different proton ordering in hexagonal ice due to their inadequate description of higher-order multipoles. Reducing the number of multipole sites from three to one requires significantly less computational effort in the iterative solution of the polarization equations. At the same time, it makes the model conceptually simpler since atomic multipole moments of molecules are poorly defined and not experimentally measurable, while the gas-phase molecular multipoles can be obtained from experiments or from ab initio calculations. In SCME, the electrostatic multipole expansion, which is switched off at short range using damping functions, is combined with a dispersion energy expression including C_6, C_8, and C_{10} coefficients derived from ab initio calculations and an empirical density-dependent isotropic short-range repulsion energy, both centered on the oxygen atom. Promising results were obtained in the description of water clusters, ice, and liquid water,[213] although some shortcomings of the SCME model are apparent in the comparisons shown in Figure 4.

To provide the reader with a general overview of the accuracy with which different implicit polarizable models describe the properties of liquid water, a compendium of structural, energetic, and thermodynamic quantities extracted from the original references is reported in Table 2. In general, all models correctly describe both density and enthalpy of vaporization at room temperature, albeit noticeable variations in their performance are observed for various other properties, with percentage deviations from the reference data being, in some cases, larger than 10%. In particular, the heat capacity and dielectric constant appear to be the properties more difficult to reproduce.

More direct comparisons are made in Figure 4, where predictions for interaction energies of the low-lying hexamer isomers and the oxygen–oxygen radial distribution function of the liquid at ambient conditions are analyzed for the most recent polarizable models with flexible monomers. The hexamer cluster is specifically chosen for this comparison because it is the smallest water cluster for which the lowest energy isomers assume fully three-dimensional structures (Figure 5), which resemble the hydrogen-bonding arrangements found in the liquid and ice. Among the six polarizable PEFs, AMOEBA2014 provides the closest agreement with the interaction energies calculated at the CCSD(T)-F12 level in ref 217 using the MP2-optimized geometries of ref 218. Both the TTM3-F and GEM* PEFs correctly predict the energy order for the different isomers, with the largest absolute deviation from the CCSD(T)-F12 values being slightly more than ~1 kcal/mol. It was shown, however, that TTM3-F achieves high accuracy in the relative energies of the different isomers through some fortuitous cancellation of errors between 2B and 3B contributions.[217] Besides providing larger deviations from the reference data, the remaining three polarizable PEFs (TTM4-F, POLI2VS, and SCME) considered in this analysis also predict a different energy order compared to the CCSD(T)-F12 results.

The comparison between the oxygen–oxygen radial distribution functions calculated from classical molecular dynamics simulations and the corresponding experimental results derived from X-ray scattering measurements of liquid water at ambient conditions[108] indicates that all six polarizable force fields overestimate the height of the first peak. It should be noted, however, that the shape of this peak, associated with molecules located in the first hydration shell, is sensitive to nuclear quantum effects which are neglected in classical molecular dynamics simulations.[219] While all six polarizable force fields correctly reproduce outer hydration shells at larger water–water separations, the current version of GEM* and the TTM4-F model predict a too weakly and too strongly structured liquid, respectively.

A quantitative assessment of the strengths and weaknesses of the current version of the SCME PES can be derived from the analysis of the lower-order terms contributing to the overall interaction energy. Figure 6a shows the absolute difference between the SCME and CCSD(T) two-body energies, $E_{\mathrm{SCME}} - E_{\mathrm{CCSD(T)}}$, calculated as a function of the oxygen–oxygen distance for a set of 27029 dimers extracted from path-integral molecular dynamics (PIMD) simulations performed with the many-body HBB2-pol potential energy function.[191] While SCME predicts accurate energetics for monomer separations larger than ~3.5 Å, large deviations from the CCSD(T) reference data are found at short range. This short-range error is associated with the breakdown of the multipole expansion as the electron clouds of neighboring monomers start to overlap and reveals deficiencies in the multipolar damping functions together with the isotropic exchange-repulsion energy model adopted by SCME. While a systematic improvement of the damping functions is possible,[220] a potentially more efficient route to describe quantum mechanical effects (e.g., exchange-repulsion and charge transfer) at short range is to replace the current empirical repulsion energy with an explicit many-body potential obtained from the application of machine-learning techniques (see section 4.3). Figure 6b shows the correlation between 3B energies obtained from SCME and CCSD(T) calculations for a set of 12347 trimer geometries.[144] Since the short-range repulsion is partially canceled from the 3B energies, the SCME results are in relatively good

agreement with the reference data. For illustrative purposes, a comparison between SCME three-body energies calculated by neglecting the induced quadrupole moments and the corresponding CCSD(T) reference data is also shown in Figure 6b. This comparison suggests that inducing the quadrupole moments may be important to enhance the binding energy for a large range of strongly hydrogen-bonded trimer geometries. However, since both AMOEBA and TTM4-F achieves high accuracy in the representation of 3B interactions by only employing inducible dipole moments (Figure 2), the role played by inducible quadrupole moments appears to be related to the specific electrostatic scheme adopted by individual PEFs (such as SCME) and merits more systematic comparative analysis.

4.3. Explicit Many-Body Potential Energy Functions

Since the MBE converges rapidly for water,[30,31,84,85,221,222] eq 1 suggests that it is possible to effectively express the energy of systems containing N water molecules in terms of low-order interactions, which, in turn, can be calculated with high accuracy using correlated electronic structure [e.g., CCSD(T)] methods. On the basis of this observation and building upon the MCY pairwise potential energy function described in section 4.1, the first many-body PEF for water with rigid monomers was developed by Niesar et al.[223,224] This PEF contains explicit 2B and 3B terms derived respectively from fourth-order Möller-Plesset (MP4) and HF calculations, along with a classical description of higher-body polarization interactions.

Subsequent improvements in the SAPT methodology enabled the development of a new global PEF (SAPT-5s+3B) for water with rigid monomers, including explicit 2B and 3B terms.[225–227] The new analytical 3B term was obtained from a fit to 7533 trimer energies calculated at the Hartree–Fock level using the SAPT formalism. SAPT-5s+3B was shown to accurately reproduce the vibration–rotation tunneling (VRT) spectrum of both $(H_2O)_2$ and $(D_2O)_2$ dimers as well as the second virial coefficient and the far-infrared spectrum of the water trimer. These studies eventually led to the development of the rigid-monomer CC-pol family of water PESs,[228–233] whose latest version, CC-pol-8s, is a 25-site model with explicit 2B and 3B terms fitted to CCSD(T)-corrected MP2 dimer energies and SAPT trimer energies, respectively. All higher-order interactions in CC-pol are represented through classical polarization. CC-pol accurately reproduces the VRT spectrum of the water dimer and predicts the structure of liquid water in reasonable agreement with the experimental data. Within the CC-pol scheme, a refined 2B term with explicit dependence on the monomer flexibility, CC-pol-8s/f, has recently been reported.[234] As shown in Figure 7a, CC-pol-8s/f reproduces the interaction energies of more than 40000 water dimers calculated at the CCSD(T)/CBS level of theory with a root-mean-square deviation (RMSD) of 0.42 kcal/mol per dimer and the experimental VRT spectrum with high accuracy (Table 3).

The first global full-dimensional water PEF (WHBB) was reported by Wang et al.[54,235–238] As in the TTM PEFs, the 1B term of WHBB is described by the spectroscopically accurate monomer PEF developed by Partridge and Schwenke,[197] while the 2B and 3B terms were fitted to CCSD(T) and MP2 data, respectively, using permutationally invariant polynomials.[239] All long-range many-body effects in WHBB are represented by the same Thole-type polarizable model used in the TTM3-F model.[40] In combination with the many-

body PES, a two-body dipole moment surface for water was also reported as part of the WHBB suite.[54,235,236] To date, WHBB has been applied to dynamical calculations of several properties of water clusters, including energies[240,241] and free energies,[242] as well as in static calculations of the vibrational frequencies of clusters,[243,244] liquid water,[245,246] and ice.[247] WHBB reproduces the CCSD(T)/CBS interaction energies of the dimer data set of ref 191 with an RMSD of 0.15 kcal/mol per dimer (Figure 7b) and predicts vibrational transitions in excellent agreement with the experimental VRT spectrum (Table 3). Although WHBB is highly accurate for very small water clusters, its accuracy appears to deteriorate as the system size increases as demonstrated by the poor agreement obtained with CCSD(T) and quantum Monte Carlo (QMC) reference data for the hexamer isomers and liquid configurations.[217] As discussed in ref 217, this lack of transferability of WHBB from small clusters to condensed-phase systems is possibly related to inaccuracies in the specific functional form adopted to merge explicit short-range and effective long-range many-body interactions.

Building upon the results obtained with CC-pol and WHBB, the full-dimensional HBB2-pol many-body PEF was introduced by Babin et al. in ref 55. As in the TTM and WHBB PESs, the 1B term of HBB2-pol is described by monomer PEF developed by Partridge and Schwenke.[197] The 2B interaction at short range is represented by the HBB2 potential,[235] which smoothly transitions at long-range into the sum of two separate terms describing electrostatic and dispersion energy interactions. The induction contributions to nonpairwise additive interactions in HBB2-pol are taken into account through Thole-type point polarizable dipoles on all atomic sites using the TTM4-F scheme.[41] In addition, an explicit 3B component is used to account for short-range interactions, such as exchange-repulsion and charge transfer. The inclusion of induction interactions at all monomer separations in the 3B term of HBB2-pol enables the use of lower degree permutationally invariant polynomials than previously reported for WHBB, resulting in a sizable decrease in the computational cost associated with both energy and force calculations. HBB2-pol is the first full-dimensional analytical PES that accurately predicts the properties of water from the gas to the condensed phase, reproducing the second and third virial coefficients, the relative energies of small water clusters, and both structural and dynamical properties of liquid water.[55] From the analysis of the HBB2-pol oxygen–oxygen radial distribution function, it was found that the inclusion of explicit 3B short-range effects is critical to correctly reproduce the structure of liquid water at ambient conditions. Moreover, HBB2-pol simulations performed using path-integral molecular dynamics combined with the replica exchange method were shown to predict the correct relative stability of $(H_2O)_6$ and $(D_2O)_6$ clusters over a wide range of temperatures.[248]

A new full-dimensional many-body PEF, MB-pol, has recently been introduced Babin et al. and shown to achieve unprecedented accuracy in predicting the properties of water across different phases.[144,191,249] The MB-pol functional form includes the 1B term by Partridge and Schwenke[197] as well as explicit 2B and 3B terms derived from large data sets of dimer and trimer interaction energies calculated at the CCSD(T) level of theory in the complete basis set limit.[144,191,249] All higher-body terms in MB-pol are represented by many-body polarization using a slightly modified version of the induction scheme adopted by the TTM4-F PEF.[41] MB-pol can thus be viewed as a flexible polarizable model supplemented

by short-range 2B and 3B terms that take effectively into account quantum-mechanical interactions arising from the overlap of the monomer electron densities. MB-pol thus contains many-body effects at all monomer separations as well as at all orders, in an explicit way up to the third order and in a mean-field fashion at higher orders. As shown in Figure 7c, MB-pol reproduces the CCSD(T)/CBS interaction energies of more than 40000 water dimer with an RMSD of 0.05 kcal/mol per dimer, which reduces to 0.03 kcal/mol for dimer with energies below 25 kcal/mol. Similarly to CC-pol-8s/f and WHBB, MB-pol reproduces the experimental VRT spectrum of the water dimer with high accuracy (Table 3). MB-pol correctly reproduces the second virial coefficient,[191] the relative energies of small water clusters,[144] and the structural, thermodynamic, and dynamical properties of liquid water at ambient conditions.[249] A recent analysis[217] of the water properties from the gas to the liquid phase shows that MB-pol predicts interaction energies and vibrational frequencies for small water clusters in close agreement with the reference values obtained from highly correlated electronic structure calculations[250] as well as the energetics of liquid configurations in agreement with quantum Monte Carlo reference data.[251] Importantly, the analysis reported in ref 217 also demonstrates that MB-pol achieves higher accuracy in the description of liquid configurations than existing DFT models that are commonly used in ab initio molecular dynamics simulations of water (see Figures 8,9, and 10).

An alternative approach to the permutationally invariant polynomials that are used to describe 2B and 3B interactions in the WHBB,[54,235–238] HBB2-pol,[55] and MB-pol[144,191,249] PEFs is represented by the Gaussian process regression, also known as krieging or kernel ridge regression.[252,253] In this method, a (typically high-dimensional) function is expressed as a linear combination of nonlinear basis functions (often Gaussians) that are centered on the actual data points. The Gaussian Approximation Potential (GAP)[254,255] framework uses this method to generate PEFs, utilizing both ab initio energies and gradients in a consistent and essentially parameter-free manner. In the case of small molecules, the GAP basis functions are rotationally invariant because the molecule geometry is described by internuclear distances and are made permutationally invariant by averaging them over the permutational symmetry group.

GAP was used to generate a 12-dimensional potential energy surface for the water dimer based on 9000 configurations with an RMS error <0.01 kcal/mol. When combined with a description of the beyond-2-body terms based on BLYP calculations and the Partridge-Schwenke model for the 1B term, the GAP PES achieved a relative RMS error <0.1 kcal/mol for the hexamer isomers.[194] However, the absolute binding energy errors were found to be significantly larger (0.3 kcal/mol for hexamers and 0.6 kcal/mol pentadecamers), due to the cooperative effects discussed in section 4.2, which are poorly described at the DFT/BLYP level (see Figure 9).[195] Similarly, relative binding energies of ice phases within the GAP model were found to be accurate (<0.1 kcal/mol) although the model systematically overestimates the binding energies by ~1.5 kcal/mol due to the overpolarisation associated with the BLYP functional. Changing the description of the many-body terms to the PBE exchange-correlation functional was found to have a somewhat remarkable effect: while PBE gives an intrinsically better description of the 2B terms, its description of the beyond-2-body terms is significantly worse than BLYP, leading to relative errors on the order of 3 kcal/mol for ice phases and clusters derived from ice-like

configurations.[196] These observations provide some possible explanations for the persistent failure of commonly used DFT models in accurately describing the properties of water.

Following the same strategy adopted to derive the HBB2-pol[32,55] and MB-pol[144,191,249] PEFs, the GAP approach has recently been used to correct the shortcomings of the polarizable SCME model (see section 4.2) in the representation of short-range 2B and 3B interactions. The resulting SCME/GAP PEF contains 2B and 3B GAP corrections derived from fits to the CCSD(T) 2B energies of ref 256 and to the same CCSD(T)/CBS 3B energies used to optimize the 3B permutationally invariant polynomials of the MB-pol PEF, respectively.[144] Although the SCME/GAP model is still under development, preliminary results shown in Figures 8 and 9 indicate that the addition of the short-range GAP corrections significantly improves the ability of the original SCME model to predict both the energetics and the individual many-body contributions to the interaction energies of the hexamer isomers.

Similar to section 4.2, the interaction energies of the hexamer isomers calculated with several many-body PEFs are analyzed in Figure 8. To provide the reader with a quantitative assessment of the accuracy of existing many-body PEFs, direct comparisons with the corresponding quantities obtained from ab initio calculations are also reported. In Figure 8a, the interaction energies of the eight low-lying hexamer isomers calculated with the SCME/GAP, WHBB, and MB-pol PEFs are compared with the corresponding CCSD(T)-F12/VTZ-F12 reference values of ref 217. All three many-body PEFs predict the correct energy order, with SCME/GAP and MB-pol providing the closest agreement with the CCSD(T)-F12/VTZ-F12 values for all isomers.

To put the results obtained with many-body PEFs in perspective, comparisons between the CCSD(T)-F12/VTZ-F12 interaction energies and the corresponding values calculated using seven popular DFT models (without and with the D3 dispersion correction[257]) commonly used in computer simulations of water are shown in Figure 8 (panels b and c). All DFT calculations were carried out with Gaussian 09[258] using the aug-cc-pVQZ basis set. The analysis of Figure 8b clearly shows that among the seven functionals without the D3 dispersion correction, only M062X and ωB97X predict the correct energy order of the hexamer isomers. However, the deviations from the CCSD(T)-F12/VTZ-F12 reference data can be as large as 6 kcal/mol, which is significantly larger than the differences obtained with all three many-body PEFs. Although the addition of the D3 dispersion correction[257] improves the agreement with the CCSD(T)-F12/VTZ-F12 values, none of the DFT models considered in this analysis achieves the same accuracy as SCME/GAP and MB-pol.

A more quantitative assessment of the accuracy of both many-body PEFs and DFT models, the many-body decomposition of the interaction energy for the prism (isomer 1), cage (isomer 2), and cyclic chair (isomer 6) hexamers is reported in Figure 9. Specifically, the errors ($\Delta E = \Delta E_{\mathrm{nB}}^{\mathrm{model}} - E_{\mathrm{nB}}^{\mathrm{CCSD(T)}}$) relative to the CCSD(T)-F12/VTZ-F12 reference values reported in ref 217 were calculated for each term (from 2B to 6B) of eq 1. The results shown in the first column of Figure 9 (panels a, d, and g) indicate that all many-body PEFs closely reproduce the reference values for each term of the MBE. However, non-negligible deviations in the 3B and 4B terms, which become more apparent for the cyclic chair isomer,

result in WHBB being overall less accurate than the SCME/GAP and MB-pol at reproducing the hexamer interaction energies as shown in Figure 8. On the other hand, large deviations from the reference data are found, especially at the 2B level, when the calculations are carried out with DFT models without the dispersion correction (panels b, e, and h of Figure 9). In this case, the PBE and PBE0 functionals provide the closest agreement with the CCSDT(T)-F12/VTZ-F12 values, although the associated errors are appreciably larger than those obtained with explicit many-body PEFs. Overall, the inclusion of the D3 dispersion correction improves the description of the 2B contributions (panels c, f, and i of Figure 9). However, while the dispersion correction improves significantly the accuracy of the BLYP functional, both PBE-D3 and PBE0-D3 2B terms become less accurate than those obtained with the original functionals. Since the D3 dispersion correction is strictly pairwise additive, it does not improve the description of higher-order interaction terms, which are found to deviate from the CCSD(T)-F12 reference values by as much as 2 kcal/mol. Interestingly, both M062X and M062X-D3 appear to benefit fortuitous error cancellation between even- and odd-order interaction terms. Among all functionals considered in this analysis, ωB97XD provides the most accurate description of each term of the MBE, independently of the isomer. However, the deviations from the CCSD(T)-F12 reference values associated with ωB97XD are still noticeably larger than those found with the WHBB, SCME/GAP, and MB-pol many-body PEFs.

Particularly remarkable is the close similarity between the results obtained with the SCME/GAP and MB-pol PEFs which effectively demonstrates both the accuracy and efficiency of the many-body-plus-polarization scheme originally introduced with the HBB2-pol PEF. Within this scheme, individual many-body contributions are explicitly added to a baseline energy expression that implicitly represents many-body effects through classical induction. These individual terms (e.g., 2B and 3B permutation-ally invariant polynomials for MB-pol and GAP functions for SCME/GAP) effectively correct the deficiencies of a classical representation of the interaction energies, recovering quantum-mechanical effects such as exchange-repulsion and charge transfer. Since MB-pol and SCME/GAP use different induction schemes and short-range corrections, the close agreement between the MB-pol and SCME/GAP results thus demonstrates that the many-body-plus-polarization scheme is robust with respect to the specific functional form adopted by the individual PEFs. Interestingly, SCME/GAP uses the same trimer training set as MB-pol to effectively achieve the same accuracy in the representation of 3B interaction energies, which emphasizes the importance of shared databases of high-quality electronic structure data for developing accurate analytical PEFs. It should also be noted that, although current implementations of many-body-plus-polarization scheme such as HBB2-pol, MB-pol, and SCME/GAP include explicit corrections up to the 3B level, this choice only represents the optimal compromise between accuracy and computational efficiency. By construction, the many-body-plus-polarization scheme is not limited by the number of MBE terms that can be included in the energy expression nor by the order of permutationally invariant polynomials (for HBB2-pol and MB-pol) and number of Gaussian functions (for SCME/GAP).

While, as of today, SCME/GAP has not been applied to any water system in periodic boundary conditions, the accuracy of WHBB and MB-pol has been further assessed in ref 217 through a direct comparison with quantum Monte Carlo interaction energies calculated

for liquid water configurations extracted from path-integral molecular dynamics simulations carried out with the vdW-DF and vdW-DF2 functionals.[251] The comparison of ref 217, shown in Figure 10a, also includes the corresponding results obtained in refs 251 and 217 for several DFT models and the TTM3-F and TTM4-F polarizable force fields, respectively. QMC has been shown to be a reliable benchmark in the study of small water clusters, producing relative energies with an accuracy comparable to that of CCSD(T). As a measure of accuracy, the mean absolute deviation (MAD) between the energies $E_{\mathrm{i}}^{(\mathrm{PES})}$ obtained with each PES and the reference QMC energies $E_{\mathrm{i}}^{(\mathrm{QMC})}$ was calculated in ref 217 as

$$\mathrm{MAD}=\frac{1}{N_{\mathrm{c}}}\sum_{i=1}^{N_{\mathrm{c}}}|(E_{\mathrm{i}}^{(\mathrm{PES})}-E_{\mathrm{i}}^{(\mathrm{QMC})})-\langle E^{(\mathrm{PES})}-E^{(\mathrm{QMC})}\rangle| \quad (6)$$

In eq 6, N_{c} is the total number of water configurations used in the analysis and $\langle E^{(\mathrm{PES})}-E^{(\mathrm{QMC})}\rangle=\frac{1}{N_{\mathrm{c}}}\sum_{i=1}^{N_{\mathrm{c}}}(E_i^{(\mathrm{PES})}-E_i^{(\mathrm{QMC})})$ is the average energy difference for all N_{c} configurations, which is used to effectively align the zero of energy with the reference QMC data. As discussed in detail in ref 217, the comparison with the QMC results demonstrates that MB-pol provides a highly accurate description of the energetics of liquid water, outperforming both current DFT and existing analytical PEFs. Figure 10a also shows that the accuracy of WHBB deteriorates for liquid configurations, leading to an MAD value relative to the QMC reference data which is ~15 times larger than MB-pol and ~4 times larger than the corresponding values obtained with the TTM3-F and TTM4-F polarizable force fields. It should be noted, however, that, as shown by the analyses presented in Figure 8 and in ref 217, fortuitous cancellation of errors between different terms of the many-body expansion of the interaction energy may also affect the energetics of the liquid configurations calculated using both DFT models and polarizable force fields.

Since molecular dynamics simulations of liquid water with WHBB are currently unfeasible due to the associated computational cost,[217] Figure 10 (panels b and c) shows the oxygen–oxygen radial distribution functions calculated from classical molecular dynamics simulations of liquid water at ambient conditions using both the MB-pol many-body potential energy function and several DFT models with and without dispersion corrections. These comparisons further demonstrate the accuracy of MB-pol, which predicts the structure of water in excellent agreement with that derived from X-ray scattering measurements. The small differences between the experimental and MB-pol results seen in the first peak of the oxygen–oxygen radial distribution function are associated with nuclear quantum effects, which are quantitatively recovered in path-integral molecular dynamics simulations with MB-pol as shown in ref 249. It is now well-established that GGA functionals (e.g., BLYP and PBE) predict a too-structured liquid. The agreement between the DFT results and the experimental data improves when dispersion corrections and/or Hartree–Fock exchange is added to the functional. However, as Figure 10 (panels b and c) shows, independently of the specific details of the functional, noticeable differences still exist between the DFT and

experimental results, with the former consistently predicting a too short oxygen–oxygen distance between molecules in the first solvation shell.

To characterize the accuracy of MB-pol in a more quantitative way, we use a new scoring scheme that has recently been introduced to compare the performance of DFT models in reproducing different water properties.[259] This scheme was used to assign a percentage score to several DFT models according to their performance in reproducing the properties of the water monomer, dimer, and hexamer, as well as of ice structures. Specifically, the properties considered in the analysis of ref 259 are the harmonic frequency of the monomer symmetric stretch ($f_{\mathrm{ss}}^{\mathrm{mono}}$), the dimer binding energy ($E_{\mathrm{b}}^{\mathrm{dim}}$), the binding energy per monomer of the cyclic-chair isomer (isomer 6 of Figure 5) of the hexamer cluster ($E_{\mathrm{b}}^{\mathrm{ring}}$), the sublimation energy of ice $\mathrm{I_h}$ ($E_{\mathrm{sub}}^{\mathrm{I_h}}$), the difference per monomer between the binding energies of the prism (isomer 1 of Figure 5) and cyclic-chair (isomer 6 of Figure 5) isomers of the hexamer cluster ($\Delta E_b^{\mathrm{prism-ring}}$), the difference of the sublimation energies of ice $\mathrm{I_h}$ and ice VIII ($\Delta E_{\mathrm{sub}}^{\mathrm{I_h-VIII}}$), the equilibrium oxygen–oxygen distance of the dimer ($R_{\mathrm{OO}}^{\mathrm{dim}}$), and the equilibrium volumes per monomer of ice $\mathrm{I_h}$ ($V_{\mathrm{eq}}^{\mathrm{Ih}}$) and ice VIII ($V_{\mathrm{eq}}^{\mathrm{VIII}}$). The scores are assigned by considering the deviations from the corresponding reference data obtained from high-level electronic structure calculations or experimental measurements. A score of 100% is assigned if the magnitude of the deviation is less than a predefined tolerance δx_{tol}, and a deduction of 10% is applied for each successive increment δx_{tol} in $|x - x_{\mathrm{ref}}|$. A zero score is given if $|x - x_{\mathrm{ref}}| > 11\ \delta x_{\mathrm{tol}}$. The interested reader is referred to ref 259 for a detailed discussion of the specific values of δx_{tol} for the different water properties. As shown in Table 4, MB-pol scores 90% or higher for all properties except for the equilibrium volume per monomer of ice VIII, outperforming all DFT models considered in ref 259. The average score for MB-pol is 93% using the reference values reported in the original analysis of ref 259, which becomes 96% if more accurate reference values for the harmonic frequency of the monomer symmetric stretch and oxygen–oxygen distance in the water dimer are considered. In addition, as shown in Table 5, molecular dynamics simulations of liquid water at ambient conditions carried out with MB-pol at both classical and quantum mechanical levels predict thermodynamic and dynamical properties in excellent agreement with the corresponding experimental values.[90,249]

On the basis of a systematic analysis of the convergence of the electrostatic properties of water,[260] full-dimensional many-body representations for the dipole moment (MB-μ) and polarizability (MB-α) have also been developed and used in combination with the MB-pol PEF to perform many-body molecular dynamics (MB-MD) simulations of the vibrational (infrared and Raman) spectra of liquid water as well as of sum-frequency generation (SFG) spectra of the air/water interface.[90,261,262] In both cases, good agreement with the experimental results is found across the entire frequency range (Figure 11). Direct comparisons with the experimental spectra demonstrate that, while an accurate description of many-body interactions is required to correctly model the (vibrational) structure of liquid water, the explicit treatment of nuclear quantum effects in the simulations is necessary to correctly capture zero-point energy effects. Importantly, as shown in Figure 11 and discussed in detail in refs 261 and 90, while MB-MD simulations using the MB-pol PEF combined

with the MB-μ and MB-α many-body representations of the water dipole moment and polarizability correctly reproduce both the shifts and the shapes of the main spectroscopic features, a more rigorous treatment of quantum dynamical effects, such as Fermi resonances and high-frequency anharmonic vibrations, is needed for bringing the stimulated spectra in quantitative agreement with the experimental measurements.

While employing an accurate PEF is the obvious requirement for a physically correct molecular-level description of the water properties, the optimal balance between accuracy and efficiency often is the ultimate criterion that dictates which PEF to use in actual simulations, since the computational cost associated with each PES directly determines the ability to calculate statistically converged quantities. To provide the reader with general estimates of the computational cost associated with the different classes of PEFs analyzed in this review, Table 6 shows the results of a performance analysis, originally reported in ref 217, carried out on a single Intel Xeon E5-2640 processor for a system consisting of 256 water molecules in periodic boundary conditions. This comparison shows that MB-pol achieves high accuracy at a cost of ~50× that of an empirical pairwise additive PEF such as q-TIP4P/F and ~6× that of an implicit many-body (i.e., polarizable) PEF such as TTM3-F.

The analysis of explicit many-body PEFs clearly demonstrates that the MBE shown in eq 1 can effectively be used to construct highly accurate representations of the water interactions rigorously derived from correlated electronic structure data. MB-pol is the first, and currently only, successful example, of such PEFs which, correctly representing many-body effects at both short and long ranges, consistently predicts the properties of water with unprecedented accuracy from the gas to the condensed phase.

5. CONCLUSIONS AND FUTURE DIRECTIONS

We have reviewed the current status of analytical potential energy functions for molecular-level computer simulations of water across different phases. Starting from simple pairwise additive functions, specific emphasis has been put on recent developments focusing on a correct description of many-body effects. Thanks to the improved understanding of hydrogen-bonding and weak interactions, which has been accompanied in the past decade by progress in algorithms for molecular simulations and increased computing power, inclusion of many-body effects either implicitly, through the addition of induction terms, or explicitly, through the addition of separate terms to the energy expressions, has become routine.

While the parametrization of many-body PEFs based on experimental data is still common and effectively appears to be the most promising approach for the development of coarse-grained models (e.g., the mW model[100]), the use of large sets of ab initio data in the fitting procedure is gaining appeal. In particular, fits to highly correlated electronic structure data, which can now be obtained at the “gold standard” CCSD(T) level for small water clusters,[218,250,263–266] represent a viable route to the development of transferable and accurate many-body PEFs. Different schemes are currently used to cast the information encoded in the ab initio data into mathematical expressions that can be both easily implemented and efficiently computed. Following earlier work on polarization effects (e.g., see ref 267 for a recent review), several water models have been developed which represent

many-body effects through induction interactions described by various schemes, including inducible point dipoles (e.g., AMOEBA,[39,141–143,268] TTM,[40,41,192–196] DDP2,[206] POLIR,[207] and POLI2VS[208]), charge-on-spring models (e.g., SWM,[134–136] COS,[137–139] and BK3[140]), and multipolar expansions (e.g., ASP-W and SCME). While these models exhibit higher transferability than effective pairwise force fields (e.g, TIPnP[56–58] and SPC∗[59,60]), they are still limited in the ability of consistently reproducing the properties of water from the gas to the condensed phase.

The limitations of polarizable PEFs can be traced to the difficulty of correctly representing both short-range interactions associated with quantum-mechanical effects (e.g., exchange-repulsion and charge transfer which arise from the overlap of the monomer electron densities) and long-range interactions that depend on the monomer properties (e.g., dipole moment and polarizability) through classical expressions describing electrostatic, repulsion, and dispersion contributions. A more physically correct description of the interaction energy can be obtained by employing schemes based on the decomposition of the ab initio energy into individual contributions. Following this approach, the SIBFA,[174–177] GEM,[145] and GEM∗[186–189] models are constructed from a systematic reproduction of each energy term, which generally leads to a more accurate description of the intermolecular interaction especially at medium to short range.

Due to its rapid convergence for water, the many-body expansion of the interaction energy can be directly used to develop many-body analytical PEFs that express the energy of systems containing N water molecules as an explicit sum over all individual interaction terms derived from highly correlated electronic structure calculations. CC-pol,[228–234] WHBB,[54,235–238] HBB2-pol,[55] SCME/GAP, and MB-pol[144,191,249,261] are recent examples of explicit many-body PEFs which, containing explicit 1B, 2B, and 3B terms supplemented by many-body induction, exhibit a high degree of transferability from small clusters in the gas phase to the liquid phase. Different mathematical functions, including permutationally invariant polynomials[239] and Gaussian approximation potentials,[254] have been used to reproduce the multidimensional complexity of 2B and 3B interactions, especially at short range.

As shown in Figures 8–10 and Tables 4 and 5, the MB-pol PEF consistently reproduces with extremely high accuracy the vibration–rotation tunneling spectrum of the water dimer, the energetics of small clusters, and the structural, thermodynamic, dynamical, and spectroscopic properties of liquid water explicitly including nuclear quantum effects. Comparisons with quantum Monte Carlo reference data also indicates that MB-pol predicts the energetics of liquid configurations and ice phases with higher accuracy than DFT models commonly used in water simulations.[217] A systematic analysis of many-body effects performed with the MB-pol PEF as a function of the system size shows that both the explicit inclusion of short-range representations of two-body and three-body effects into the potential energy function and a physically correct incorporation of short- and long-range contributions are necessary for an accurate representation of the water interactions from the gas to the condensed phase.[217]

As stated in ref 269, “If the ultimate goal of simulations is to predict reliably, not reproduce, experimental results, then simulations must be built on physically justifiable models”. In this context, the development of many-body potential energy functions certainly represents a major step toward the long-sought “universal model” capable of describing the behavior of water under different conditions and in different environments. However, significant challenges, both theoretical and computational, remain which should be addressed in the future before many-body approaches can become common practice in molecular simulations of aqueous systems. First, the nonstandard expressions used to explicitly describe individual terms of the many-body expansion of the interaction energy (e.g., 2B and 3B contributions) require the development of specialized software. Although progress in this direction has been made with the implementation of the MB-pol PEF as an independent plugin for the reference platform of the OpenMM toolkit,[270] the availability of functionalities for the explicit treatment of many-body terms in common software for molecular simulations is extremely limited. Considering the algorithmic complexity of some of the mathematical functions used to describe many-body interactions, future collaborations between theoretical/computational chemists/physicists and computer scientists are desirable for the development of efficient software that can take full advantage of modern hardware. Importantly, as demonstrated by the similar accuracy achieved by SCME/GAP and MB-pol, building shared databases of high-quality electronic structure data will be critical to the development of accurate many-body PEFs for generic aqueous systems. Efforts along these lines are already ongoing.

Second, by construction, a many-body PEF is designed to represent the underlying Born–Oppenheimer potential energy surface, which implies that nuclear quantum effects should be explicitly included in the actual molecular simulation. Efficient algorithms to effectively take into account nuclear quantum effects through the application of colored-noise thermostats[271,272] and ring-polymer contraction schemes[273] have recently been proposed and should be investigated within the many-body formalism (see the review article in this thematic issue devoted specifically to nuclear quantum effects in water[71]).

Third, exploration of the transferability of many-body approaches to complex (heterogeneous) aqueous systems has only recently begun.[274–281] Although initial results for ion–water clusters are promising, the generalization to aqueous solutions of arbitrary complexity requires further theoretical and computational developments.

Finally, with the exception of a few early attempts,[127,133] all analytical PEFs described in this review enforce the water molecules to maintain their distinct molecular nature, neglecting autoionization events. While this is a good approximation for the description of pure water systems, the ability of correctly modeling the behavior of hydronium and hydroxide ions becomes increasingly important for molecular simulations of heterogeneous aqueous solutions. Ongoing work in this area is focusing on the extension of the many-body formalism to reactive representations[282] as well as on the integration of current (nonreactive) many-body potential energy functions in adaptive quantum mechanical/molecular mechanical (adQM/MM) schemes.[283–291]

Acknowledgments

This review was initiated during the Nordita (Nordic Institute for Theoretical Physics) scientific program “Water - the Most Anomalous Liquid”. Additional financial support for this program was provided by the Royal Swedish Academy of Sciences through its Nobel Institutes for Physics and Chemistry, by the Swedish Research Council, and by the Department of Physics at Stockholm University. K.T.W. was supported by The Icelandic Research Fund. J.L. and V.M. were supported by the Army Research Laboratory under Cooperative Agreement W911NF-12-2-0023. Y.X. was supported by the Cluster of Excellence RESOLV (EXC 1069) funded by the Deutsche Forschungsgemeinschaft (DFG). G.A.C. was supported by Wayne State University and the National Institutes of Health, Grant R01GM108583. F.P. was supported by the National Science Foundation through Grant CHE-1453204. Allocations of computing time from HPC2N (Sweden), NSC (Sweden), NHPC (Iceland), Wayne State University Grid Computing, the Center for High Performance Computing at The University of Utah, the Extreme Science and Engineering Discovery Environment (XSEDE), which is supported by the National Science Foundation Grant ACI-1053575, and the National Energy Research Scientific Computing Center (NERSCC), which is supported by the Office of Science of the U.S. Department of Energy under Contract DE-AC02-05CH11231, are gratefully acknowledged. A.B.P. is supported by a Leverhulme Early Career Fellowship and the Isaac Newton Trust. We are grateful to Mr. Yicun Ni and Prof. Jim Skinner for providing the E3B data[107] of Figure 4, Prof. Yoshitaka Tanimura and Dr. Taisuke Hasegawa for providing the POLI2VS code, Prof. Lee-Ping Wang, Prof. Michele Ceriotti, and Prof. Robert DiStasio for providing the classical oxygen–oxygen radial distribution functions calculated with AMOEBA2014 in ref 268, with BLYP, BLYP-D3, and B3LYP-D3 in ref 292, and with PBE, PBE-TS(vdW), PBE0, and PBE0-TS(vdW) in ref 293, respectively.

References

1. Allen, MP., Tildesley, DJ. Computer Simulation of Liquids. Oxford University Press; New York: 1987.
2. Leach, AR. Molecular Modeling: Principles and Applications. 2. Pearson Prentice Hall; New York: 2001.
3. Tuckerman, ME. Statistical Mechanics: Theory and Molecular Simulation. Oxford University Press; New York: 2010.
4. Mayo SL, Olafson BD, Goddard WA. Dreiding - A Generic Force-Field for Molecular Simulations. J Phys Chem. 1990; 94:8897–8909.
5. Cornell WD, Cieplak P, Bayly CI, Gould IR, Merz KM, Ferguson DM, Spellmeyer DC, Fox T, Caldwell JW, Kollman PA. A 2nd Generation Force Field for the Simulation of Proteins, Nucleic Acids, and Organic Molecules. J Am Chem Soc. 1995; 117:5179–5197.
6. Jorgensen WL, Maxwell DS, TiradoRives J. Development and Testing of the OPLS All-Atom Force Field on Conformational Energetics and Properties of Organic Liquids. J Am Chem Soc. 1996; 118:11225–11236.
7. Wang JM, Wolf RM, Caldwell JW, Kollman PA, Case DA. Development and Testing of a General Amber Force Field. J Comput Chem. 2004; 25:1157–1174. [PubMed: 15116359]
8. Vanommeslaeghe K, Hatcher E, Acharya C, Kundu S, Zhong S, Shim J, Darian E, Guvench O, Lopes P, Vorobyov I, MacKerell AD. CHARMM General Force Field: A Force Field for Drug-Like Molecules Compatible with the CHARMM All-Atom Additive Biological Force Fields. J Comput Chem. 2009; 31:671–690.
9. Car R, Parrinello M. Unified Approach for Molecular Dynamics and Density-Functional Theory. Phys Rev Lett. 1985; 55:2471–2474. [PubMed: 10032153]
10. Marx, D. Ab initio Molecular Dynamics: Basic Theory and Advanced Methods. Cambridge University Press; New York: 2009.
11. Del Ben M, Schoenherr M, Hutter J, VandeVondele J. Bulk Liquid Water at Ambient Temperature and Pressure from MP2 Theory. J Phys Chem Lett. 2013; 4:3753–3759.
12. Del Ben M, VandeVondele J, Slater B. Periodic MP2: RPA, and Boundary Condition Assessment of Hydrogen Ordering in Ice XV. J Phys Chem Lett. 2014; 5:4122–4128. [PubMed: 26278943]
13. Willow SY, Salim MA, Kim KS, Hirata S. Ab Initio Molecular Dynamics of Liquid Water Using Embedded-Fragment Second-Order Many-Body Perturbation Theory Towards its Accurate Property Prediction. Sci Rep. 2015; 5:14358. [PubMed: 26400690]
14. Willow SY, Zeng XC, Xantheas SS, Kim KS, Hirata S. Why Is MP2-Water “Cooler” and “Denser” than DFT-Water? J Phys Chem Lett. 2016; 7:680–684. [PubMed: 26821830]

15. Beck MH, Jackle A, Worth GA, Meyer HD. The Multiconfiguration Time-Dependent Hartree (MCTDH) Method: A Highly Efficient Algorithm for Propagating Wavepackets. Phys Rep. 2000; 324:1–105.
16. Leforestier C, Bisseling RH, Cerjan C, Feit MD, Friesner R, Guldberg A, Hammerich A, Jolicard G, Karrlein W, Meyer HD, Lipkin N, Roncero O, Kosloff R. A Comparison of Different Propagation Schemes for the Time-Dependent Schrödinger Equation. J Comput Phys. 1991; 94:59–80.
17. Miller WH. The Semiclassical Initial Value Representation: A Potentially Practical Way for Adding Quantum Effects to Classical Molecular Dynamics Simulations. J Phys Chem A. 2001; 105:2942–2955.
18. Chandler D, Wolynes PG. Exploiting the Isomorphism Between Quantum-Theory and Classical Statistical-Mechanics of Polyatomic Fluids. J Chem Phys. 1981; 74:4078–4095.
19. Marx D, Parrinello M. Ab Initio Path-Integral Molecular Dynamics: Basic Ideas. J Chem Phys. 1996; 104:4077–4082.
20. Voth GA. Path-Integral Centroid Methods in Quantum Statistical Mechanics and Dynamics. Adv Chem Phys. 1996; 93:135–218.
21. Habershon S, Manolopoulos DE, Markland TE, Miller TF. Ring-Polymer Molecular Dynamics: Quantum Effects in Chemical Dynamics from Classical Trajectories in an Extended Phase Space. Annu Rev Phys Chem. 2013; 64:387–413. [PubMed: 23298242]
22. Hankins D, Moskowitz JW, Stillinger FH. Water Molecule Interactions. J Chem Phys. 1970; 53:4544.
23. Del Bene J, Pople JA. Intermolecular Energies of Small Water Polymers. Chem Phys Lett. 1969; 4:426–428.
24. Clementi E, Kolos W, Lie GC, Ranghino G. Nonadditivity of Interaction in Water Trimers. Int J Quantum Chem. 1980; 17:377–398.
25. Yoon BJ, Morokuma K, Davidson ER. Structure of ice Ih - Ab Initio 2-Body and 3-Body Water-Water Potentials and Geometry Optimization. J Chem Phys. 1985; 83:1223–1231.
26. Kim KS, Dupuis M, Lie GC, Clementi E. Revisiting Small Clusters of Water Molecules. Chem Phys Lett. 1986; 131:451–456.
27. Hermansson K. Many-Body Effects in Tetrahedral Water Clusters. J Chem Phys. 1988; 89:2149–2159.
28. Xantheas SS, Dunning TH. The Structure of the Water Trimer from Ab Initio Calculations. J Chem Phys. 1993; 98:8037–8040.
29. Ojamae L, Hermansson K. Ab Initio Study of Cooperativity in Water Chains. Binding Energies and Anharmonic Frequencies. J Phys Chem. 1994; 98:4271–4282.
30. Xantheas SS. Ab Initio Studies of Cyclic Water Clusters $(H_2O)_N$, N = 1–6. 2. Analysis of Many-Body Interactions. J Chem Phys. 1994; 100:7523–7534.
31. Góra U, Podeszwa R, Cencek W, Szalewicz K. Interaction Energies of Large Clusters from Many-Body Expansion. J Chem Phys. 2011; 135:224102. [PubMed: 22168675]
32. Medders GR, Babin V, Paesani F. A Critical Assessment of Two-Body and Three-Body Interactions in Water. J Chem Theory Comput. 2013; 9:1103–1114. [PubMed: 26588754]
33. Kendall RA, Dunning TH, Harrison RJ. Electron-Affinities of the 1st-Row Atoms Revisited - Systematic Basis-Sets and Wave-Functions. J Chem Phys. 1992; 96:6796–6806.
34. Woon DE, Dunning TH. Gaussian-Basis Sets for Use in Correlated Molecular Calculations. 3. The Atoms Aluminum Through Argon. J Chem Phys. 1993; 98:1358–1371.
35. Boys SF, Bernardi F. The Calculation of Small Molecular Interactions by Differences of Separate Total Energies - Some Procedures with Reduced Errors. Mol Phys. 1970; 19:553–566.
36. Park K, Lin W, Paesani F. A Refined MS-EVB Model for Proton Transport in Aqueous Environments. J Phys Chem B. 2012; 116:343–352. [PubMed: 22107267]
37. Habershon S, Markland TE, Manolopoulos DE. Competing Quantum Effects in the Dynamics of a Flexible Water Model. J Chem Phys. 2009; 131:024501. [PubMed: 19603998]
38. Tainter CJ, Pieniazek PA, Lin YS, Skinner JL. Robust Three-Body Water Simulation Model. J Chem Phys. 2011; 134:184501. [PubMed: 21568515]

39. Ren PY, Ponder JW. Polarizable Atomic Multipole Water Model for Molecular Mechanics Simulation. J Phys Chem B. 2003; 107:5933–5947.
40. Fanourgakis GS, Xantheas SS. Development of Transferable Interaction Potentials for Water. V. Extension of the Flexible, Polarizable, Thole-Type Model Potential (TTM3-F, v. 3.0) to Describe the Vibrational Spectra of Water Clusters and Liquid Water. J Chem Phys. 2008; 128:074506. [PubMed: 18298156]
41. Burnham CJ, Anick DJ, Mankoo PK, Reiter GF. The Vibrational Proton Potential in Bulk Liquid Water and Ice. J Chem Phys. 2008; 128:154519. [PubMed: 18433247]
42. Stewart JJP. Optimization of Parameters for Semiempirical Methods. 1. Method. J Comput Chem. 1989; 10:209–220.
43. Stewart JJP. Optimization of Parameters for Semiempirical Methods V: Modification of NDDO Approximations and Application to 70 Elements. J Mol Model. 2007; 13:1173–1213. [PubMed: 17828561]
44. Chang DT, Schenter GK, Garrett BC. Self-Consistent Polarization Neglect of Diatomic Differential Overlap: Application to Water Clusters. J Chem Phys. 2008; 128:164111. [PubMed: 18447425]
45. Murdachaew G, Mundy CJ, Schenter GK, Laino T, Hutter J. Semiempirical Self-Consistent Polarization Description of Bulk Water, the Liquid-Vapor Interface, and Cubic Ice. J Phys Chem A. 2011; 115:6046–6053. [PubMed: 21370904]
46. Becke AD. Density-Functional Exchange-Energy Approximation with Correct Asymptotic Behavior. Phys Rev A: At, Mol, Opt Phys. 1988; 38:3098–3100.
47. Lee CT, Yang WT, Parr RG. Development of the Colle-Salvetti Correlation-Energy Formula into a Functional of the Electron Density. Phys Rev B: Condens Matter Mater Phys. 1988; 37:785–789.
48. Perdew JP, Burke K, Ernzerhof M. Generalized Gradient Approximation Made Simple. Phys Rev Lett. 1996; 77:3865–3868. [PubMed: 10062328]
49. Grimme S. Semiempirical GGA-type Density Functional Constructed with a Long-Range Dispersion Correction. J Comput Chem. 2006; 27:1787–1799. [PubMed: 16955487]
50. Becke AD. Density-Functional Thermochemistry. 3. The Role of Exact Exchange. J Chem Phys. 1993; 98:5648–5652.
51. Adamo C, Barone V. Toward Reliable Density Functional Methods Without Adjustable Parameters: The PBE0Model. J Chem Phys. 1999; 110:6158–6170.
52. Vydrov OA, Van Voorhis T. Nonlocal Van der Waals Density Functional: The Simpler the Better. J Chem Phys. 2010; 133:244103. [PubMed: 21197972]
53. Car R, Galli G. Aqueous Systems from First Principles. Chem Rev. 2016 this issue.
54. Wang YM, Huang XC, Shepler BC, Braams BJ, Bowman JM. Flexible, Ab Initio Potential, and Dipole Moment Surfaces for Water. I. Tests and Applications for Clusters up to the 22-mer. J Chem Phys. 2011; 134:094509. [PubMed: 21384987]
55. Babin V, Medders GR, Paesani F. Toward a Universal Water Model: First Principles Simulations from the Dimer to the Liquid Phase. J Phys Chem Lett. 2012; 3:3765–3769. [PubMed: 26291108]
56. Jorgensen WL, Chandrasekhar J, Madura JD, Impey RW, Klein ML. Comparison of Simple Potential Functions for Simulating Liquid Water. J Chem Phys. 1983; 79:926–935.
57. Mahoney MW, Jorgensen WL. A Five-Site Model for Liquid Water and the Reproduction of the Density Anomaly by Rigid, Nonpolarizable Potential Functions. J Chem Phys. 2000; 112:8910–8922.
58. Horn HW, Swope WC, Pitera JW, Madura JD, Dick TJ, Hura GL, Head-Gordon T. Development of an Improved Four-Site Water Model for Biomolecular Simulations: TIP4P-Ew. J Chem Phys. 2004; 120:9665–9678. [PubMed: 15267980]
59. Berendsen HJC, Grigera JR, Straatsma TP. The Missing Term in Effective Pair Potentials. J Phys Chem. 1987; 91:6269–6271.
60. Berendsen, HJC., Postma, JPM., van Gunsteren, WF., Hermans, J. Interaction Models for Water in Relation to Protein Hydration. In: Pullman, B., editor. Intermolecular Forces. Reidel; Dordrecht: 1981. p. 331-342.
61. Guillot B. A Reappraisal of What We Have Learnt During Three Decades of Computer Simulations on Water. J Mol Liq. 2002; 101:219–260.

62. Vega C, Abascal JLF. Simulating Water with Rigid Non-Polarizable Models: A General Perspective. Phys Chem Chem Phys. 2011; 13:19663–19688. [PubMed: 21927736]
63. Dang LX, Pettitt BM. Simple Intramolecular Model Potentials for Water. J Phys Chem. 1987; 91:3349–3354.
64. Teleman O, Jonsson B, Engstrom S. A Molecular Dynamics Simulation of a Water Model with Intramolecular Degrees of Freedom. Mol Phys. 1987; 60:193–203.
65. Ferguson DM. Parameterization and Evaluation of a Flexible Water Model. J Comput Chem. 1995; 16:501–511.
66. Lobaugh J, Voth GA. A Quantum Model for Water: Equilibrium and Dynamical Properties. J Chem Phys. 1997; 106:2400–2410.
67. Amira S, Spangberg D, Hermansson K. Derivation and Evaluation of a Flexible SPC Model for Liquid Water. Chem Phys. 2004; 303:327–334.
68. Wu YJ, Tepper HL, Voth GA. Flexible Simple Point-Charge Water Model with Improved Liquid-State Properties. J Chem Phys. 2006; 124:024503. [PubMed: 16422607]
69. Paesani F, Zhang W, Case DA, Cheatham TE, Voth GA. An Accurate and Simple Quantum Model for Liquid Water. J Chem Phys. 2006; 125:184507. [PubMed: 17115765]
70. Gonzalez MA, Abascal JLF. A Flexible Model for Water Based on TIP4P/2005. J Chem Phys. 2011; 135:224516. [PubMed: 22168712]
71. Ceriotti M, Fang W, Kusalik PG, McKenzie RH, Michaelides A, Morales MA, Markland TE. Nuclear Quantum Effects in Water and Aqueous Systems: Experiment, Theory, and Current Challenges. Chem Rev. 2016 this issue.
72. Matsuoka O, Clementi E, Yoshimine M. CI Study of the Water Dimer Potential Surface. J Chem Phys. 1976; 64:1351–1361.
73. Evans MW, Refson K, Swamy KN, Lie GC, Clementi E. Molecular Dynamics Simulation of Liquid Water with an Ab Initio Flexible Water-Water Interaction Potential. 2. The Effect of Internal Vibrations on the Time Correlation Functions. Phys Rev A: At, Mol, Opt Phys. 1987; 36:3935–3942.
74. Slanina Z. A Comparison of BJH-Type and MCYL-Type Potentials for the Water Dimer. J Chim Phys Phys-Chim Biol. 1991; 88:2381–2386.
75. Slanina Z. Flexible BJH-Type and MCYL-Type Potentials for the Water Dimer $(H_2O)_2$(g) - A Successful Reproduction of the Observed Monomer Dimer Vibrational Frequency-Shifts. Z Phys Chem. 1991; 171:131–136.
76. Slanina Z, Crifo JF. A Refined Evaluation of the Gas-Phase Water-Dimerization Equilibrium-Constant within Nonrigid BJH-Type and MCY-Type Potentials. Int J Thermophys. 1992; 13:465–476.
77. Kolafa J, Nezbeda I. Implementation of the Dahl-Andersen-Wertheim Theory for Realistic Water-Water Potentials. Mol Phys. 1989; 66:87–95.
78. Lyubartsev AP, Laaksonen A. Determination of Effective Pair Potentials from Ab Initio Simulations: Application to Liquid Water. Chem Phys Lett. 2000; 325:15–21.
79. Honda K, Kitaura K. A New Form for Intermolecular Potential-Energy Functions. Chem Phys Lett. 1987; 140:53–56.
80. Mas EM, Bukowski R, Szalewicz K, Groenenboom GC, Wormer PES, van der Avoird A. Water Pair Potential of Near Spectroscopic Accuracy. I. Analysis of Potential Surface and Virial Coefficients. J Chem Phys. 2000; 113:6687–6701.
81. Mas EM, Szalewicz K, Bukowski R, Jeziorski B. Pair Potential for Water from Symmetry-Adapted Perturbation Theory. J Chem Phys. 1997; 107:4207–4218.
82. Jeziorski B, Moszynski R, Szalewicz K. Pertubation-Theory Approach to Intermolecular Potential-Energy Surfaces of Van der Waals Complexes. Chem Rev. 1994; 94:1887–1930.
83. Barnes P, Finney JL, Nicholas JD, Quinn JE. Cooperative Effects in Simulated Water. Nature. 1979; 282:459–464.
84. Pedulla JM, Vila F, Jordan KD. Binding Energy of the Ring Form of $(H_2O)_6$: Comparison of the Predictions of Conventional and Localized-Orbital MP2 Calculations. J Chem Phys. 1996; 105:11091–11099.

85. Hodges MP, Stone AJ, Xantheas SS. Contribution of Many-Body Terms to the Energy for Small Water Clusters: A Comparison of Ab Initio Calculations and accurate model potentials. J Phys Chem A. 1997; 101:9163–9168.

86. Xantheas SS. Cooperativity and Hydrogen Bonding Network in Water Clusters. Chem Phys. 2000; 258:225–231.

87. Watanabe K, Klein ML. Effective Pair Potentials and the Properties of Water. Chem Phys. 1989; 131:157–167.

88. Iuchi S, Izvekov S, Voth GA. Are Many-Body Electronic Polarization Effects Important in Liquid Water? J Chem Phys. 2007; 126:124505. [PubMed: 17411142]

89. Tainter CJ, Skinner JL. The Water Hexamer: Three-Body Interactions, Structures, Energetics, and OH-Stretch Spectroscopy at Finite Temperature. J Chem Phys. 2012; 137:104304. [PubMed: 22979856]

90. Medders GR, Paesani F. Dissecting the Molecular Structure of the Air/Water Interface from Quantum Simulations of the Sum-Frequency Generation Spectrum. J Am Chem Soc. 2016; 138:3912–3919. [PubMed: 26943730]

91. Poole PH, Sciortino F, Grande T, Stanley HE, Angell CA. Effect of Hydrogen Bonds on the Thermodynamic Behavior of Liquid Water. Phys Rev Lett. 1994; 73:1632–1635. [PubMed: 10056844]

92. Jagla EA. Phase Behavior of a System of Particles with Core Collapse. Phys Rev E: Stat Phys, Plasmas, Fluids, Relat Interdiscip Top. 1998; 58:1478–1486.

93. Jagla EA. Core-Softened Potentials and the Anomalous Properties of Water. J Chem Phys. 1999; 111:8980–8986.

94. Truskett TM, Debenedetti PG, Sastry S, Torquato S. A Single-Bond Approach to Orientation-Dependent Interactions and its Implications for Liquid Water. J Chem Phys. 1999; 111:2647–2656.

95. Franzese G, Malescio G, Skibinsky A, Buldyrev SV, Stanley HE. Generic Mechanism for Generating a Liquid-Liquid Phase Transition. Nature. 2001; 409:692–695. [PubMed: 11217853]

96. Yan Z, Buldyrev SV, Giovambattista N, Stanley HE. Structural Order for One-Scale and Two-Scale Potentials. Phys Rev Lett. 2005; 95:130604. [PubMed: 16197129]

97. Xu L, Buldyrev SV, Angell CA, Stanley HE. Thermodynamics and Dynamics of the Two-Scale Spherically Symmetric Jagla Ramp Model of Anomalous Liquids. Phys Rev E. 2006; 74:031108.

98. Buldyrev SV, Kumar P, Debenedetti PG, Rossky PJ, Stanley HE. Water-Like Solvation Thermodynamics in a Spherically Symmetric Solvent Model with Two Characteristic Lengths. Proc Natl Acad Sci U S A. 2007; 104:20177–20182. [PubMed: 18077365]

99. Bizjak A, Urbic T, Vlachy V, Dill KA. The Three-Dimensional “Mercedes Benz” Model of Water. Acta Chim Slov. 2007; 54:532–537.

100. Molinero V, Moore EB. Water Modeled as an Intermediate Element between Carbon and Silicon. J Phys Chem B. 2009; 113:4008–4016. [PubMed: 18956896]

101. Noid WG. Perspective: Coarse-Grained Models for Biomolecular Systems. J Chem Phys. 2013; 139:090901. [PubMed: 24028092]

102. Johnson ME, Head-Gordon T, Louis AA. Representability Problems for Coarse-Grained Water Potentials. J Chem Phys. 2007; 126:144509. [PubMed: 17444725]

103. Larini L, Lu LY, Voth GA. The Multiscale Coarse-Graining Method. VI. Implementation of Three-Body Coarse-Grained Potentials. J Chem Phys. 2010; 132:164107. [PubMed: 20441258]

104. Stillinger FH, Weber TA. Computer Simulation of Local Order in Condensed Phases of Silicon. Phys Rev B: Condens Matter Mater Phys. 1985; 31:5262–5271.

105. Lu J, Qiu Y, Baron R, Molinero V. Coarse-Graining of TIP4P/2005, TIP4P-Ew, SPC/E, and TIP3P to Monatomic Anisotropic Water Models Using Relative Entropy Minimization. J Chem Theory Comput. 2014; 10:4104–4120. [PubMed: 26588552]

106. Kumar R, Skinner JL. Water Simulation Model with Explicit Three-Molecule Interactions. J Phys Chem B. 2008; 112:8311–8318. [PubMed: 18570461]

107. Tainter CJ, Shi L, Skinner JL. Reparametrized E3B (Explicit Three-Body) Water Model Using the TIP4P/2005 Model as a Reference. J Chem Theory Comput. 2015; 11:2268–2277. [PubMed: 26574425]

108. Skinner LB, Huang CC, Schlesinger D, Pettersson LGM, Nilsson A, Benmore CJ. Benchmark Oxygen-Oxygen Pair-Distribution Function of Ambient Water from X-Ray Diffraction Measurements with a Wide Q-Range. J Chem Phys. 2013; 138:074506. [PubMed: 23445023]
109. Shi L, Ni Y, Drews SEP, Skinner JL. Dielectric Constant and Low-Frequency Infrared Spectra for Liquid Water and Ice Ih within the E3B Model. J Chem Phys. 2014; 141:084508. [PubMed: 25173022]
110. Kitaura K, Morokuma K. New Energy Decomposition Scheme for Molecular-Interactions within Hartree-Fock Approximation. Int J Quantum Chem. 1976; 10:325–340.
111. Murrell JN, Shaw G. Effect of Overlap on Dispersion Energies Near Van der Waals Minimum. J Chem Phys. 1968; 49:4731.
112. Murrell JN, Shaw G. Intermolecular Forces in Region of Small Orbital Overlap. J Chem Phys. 1967; 46:1768.
113. Bagus PS, Hermann K, Bauschlicher CW. A New Analysis of Charge-Transfer and Polarization for Ligand-Metal Bonding-Model Studies of Al_4CO and Al_4NH_3. J Chem Phys. 1984; 80:4378–4386.
114. Stevens WJ, Fink WH. Frozen Fragment Reduced Variational Space Analysis of Hydrogen-Bonding Interactions. Application to the Water Dimer. Chem Phys Lett. 1987; 139:15–22.
115. Piquemal JP, Marquez A, Parisel O, Giessner-Prettre C. A CSOV Study of the Difference between HF and DFT Intermolecular Interaction Energy Values: The Importance of the Charge Transfer Contribution. J Comput Chem. 2005; 26:1052–1062. [PubMed: 15898112]
116. Mo YR, Gao JL, Peyerimhoff SD. Energy Decomposition Analysis of Intermolecular Interactions Using a Block-Localized Wave Function Approach. J Chem Phys. 2000; 112:5530–5538.
117. Khaliullin RZ, Head-Gordon M, Bell AT. An Efficient Self-Consistent Field Method for Large Systems of Weakly Interacting Components. J Chem Phys. 2006; 124:204105. [PubMed: 16774317]
118. Glendening ED, Streitwieser A. Natural Energy Decomposition Analysis. An Energy Paritioning Procedure for Molecular Interactions with Application to Weak Hydrogen-Bonding, Strong Ionic, and Moderate Donor-Acceptor Interactions. J Chem Phys. 1994; 100:2900–2909.
119. Lu Z, Zhou N, Wu Q, Zhang Y. Directional Dependence of Hydrogen Bonds: A Density-Based Energy Decomposition Analysis and its Implications on Force Field Development. J Chem Theory Comput. 2011; 7:4038–4049. [PubMed: 22267958]
120. Fang D, Piquemal JP, Liu S, Cisneros GA. DFT-Steric-Based Energy Decomposition Analysis of Intermolecular Interactions. Theor Chem Acc. 2014; 133:1484.
121. Hihschfelder JO. Perturbation Theory for Exchange Forces. Chem Phys Lett. 1967; 1:363–368.
122. Hesselmann A, Jansen G, Schuetz M. Interaction Energy Contributions of H-Bonded and Stacked Structures of the AT and GC DNA Base Pairs from the Combined Density Functional Theory and Intermolecular Perturbation Theory Approach. J Am Chem Soc. 2006; 128:11730–1173. [PubMed: 16953592]
123. Hesselmann A, Korona T. Intermolecular Symmetry-Adapted Perturbation Theory Study of Large Organic Complexes. J Chem Phys. 2014; 141:094107. [PubMed: 25194364]
124. Cwiok T, Jeziorski B, Kolos W, Moszynski R, Szalewicz K. Symmetry-Adapted Perturbation-Theory of Potential Energy Surfaces for Weakly-Bound Molecular Complexes. J Mol Struct: THEOCHEM. 1994; 307:135–151.
125. Parker TM, Burns LA, Parrish RM, Ryno AG, Sherrill CD. Levels of Symmetry Adapted Perturbation Theory (SAPT). I. Efficiency and Performance for Interaction Energies. J Chem Phys. 2014; 140:094106. [PubMed: 24606352]
126. Parrish RM, Sherrill CD. Spatial Assignment of Symmetry Adapted Perturbation Theory Interaction Energy Components: The Atomic SAPT Partition. J Chem Phys. 2014; 141:044115. [PubMed: 25084889]
127. Stillinger FH, David CW. Polarization Model for Water and Its Ionic Dissociation Products. J Chem Phys. 1978; 69:1473–1484.
128. Lybrand TP, Kollman PA. Water-Water and Water-Ion Potential Functions Including Terms for Many-Body Effects. J Chem Phys. 1985; 83:2923–2933.

129. Caldwell JW, Kollman PA. Structure and Properties of Neat Liquids Using Nonaddtive Molecular Dynamics: Water, Methanol, and N-Methylacetamide. J Phys Chem. 1995; 99:6208–6219.
130. Chen B, Xing JH, Siepmann JI. Development of Polarizable Water Force Fields for Phase Equilibrium Calculations. J Phys Chem B. 2000; 104:2391–2401.
131. Cho KH, No KT, Scheraga HA. A Polarizable Force Field for Water Using an Artificial Neural Network. J Mol Struct. 2002; 641:77–91.
132. Stern HA, Rittner F, Berne BJ, Friesner RA. Combined Fluctuating Charge and Polarizable Dipole Models: Application to a Five-Site Water Potential Function. J Chem Phys. 2001; 115:2237–2251.
133. Ojamäe L, Shavitt I, Singer SJ. Potential Models for Simulations of the Solvated Proton in Water. J Chem Phys. 1998; 109:5547–5564.
134. Lamoureux G, MacKerell AD, Roux B. A Simple Polarizable Model of Water Based on Classical Drude Oscillators. J Chem Phys. 2003; 119:5185–5197.
135. Lamoureux G, Harder E, Vorobyov IV, Roux B, MacKerell AD. A Polarizable Model of Water for Molecular Dynamics Simulations of Biomolecules. Chem Phys Lett. 2006; 418:245–249.
136. Yu WB, Lopes PEM, Roux B, MacKerell AD. Six-Site Polarizable Model of Water Based on the Classical Drude Oscillator. J Chem Phys. 2013; 138:034508. [PubMed: 23343286]
137. Yu HB, Hansson T, van Gunsteren WF. Development of a Simple, Self-Consistent Polarizable Model for Liquid Water. J Chem Phys. 2003; 118:221–234.
138. Yu HB, van Gunsteren WF. Charge-on-Spring Polarizable Water Models Revisited: From Water Clusters to Liquid Water to Ice. J Chem Phys. 2004; 121:9549–9564. [PubMed: 15538877]
139. Kunz APE, van Gunsteren WF. Development of a Nonlinear Classical Polarization Model for Liquid Water and Aqueous Solutions: COS/D. J Phys Chem A. 2009; 113:11570–11579. [PubMed: 19663490]
140. Kiss PT, Baranyai A. A Systematic Development of a Polarizable Potential of Water. J Chem Phys. 2013; 138:204507. [PubMed: 23742493]
141. Ponder JW, Wu C, Ren P, Pande VS, Chodera JD, Schnieders MJ, Haque I, Mobley DL, Lambrecht DS, DiStasio RA Jr, Head-Gordon M, Clark GNI, Johnson ME, Head-Gordon T. Current Status of the AMOEBA Polarizable Force Field. J Phys Chem B. 2010; 114:2549–2564. [PubMed: 20136072]
142. Ren PY, Ponder JW. Temperature and Pressure Dependence of the AMOEBA Water Model. J Phys Chem B. 2004; 108:13427–13437.
143. Wang LP, Head-Gordon T, Ponder JW, Ren P, Chodera JD, Eastman PK, Martinez TJ, Pande VS. Systematic Improvement of a Classical Molecular Model of Water. J Phys Chem B. 2013; 117:9956–9972. [PubMed: 23750713]
144. Babin V, Medders GR, Paesani F. Development of a “First Principles” Water Potential with Flexible Monomers. II: Trimer Potential Energy Surface, Third Virial Coefficient, and Small Clusters. J Chem Theory Comput. 2014; 10:1599–1607. [PubMed: 26580372]
145. Cisneros GA, Karttunen M, Ren PY, Sagui C. Classical Electrostatics for Biomolecular Simulations. Chem Rev. 2014; 114:779–814. [PubMed: 23981057]
146. Torabifard H, Starovoytov O, Ren P, Cisneros GA. Development of an AMOEBA Water Model Using GEM Distributed Multipoles. Theor Chem Acc. 2015; 134:1–10.
147. Chialvo AA, Cummings PT. Simple Transferable Intermolecular Potential for the Molecular Simulation of Water over Wide Ranges of State Conditions. Fluid Phase Equilib. 1998; 150–151:73–81.
148. Paricaud P, Predota M, Chialvo AA, Cummings PT. From Dimer to Condensed Phases at Extreme Conditions: Accurate Predictions of the Properties of Water by a Gaussian Charge Polarizable Model. J Chem Phys. 2005; 122:24451.
149. Campbell ES, Mezei M. Use of a Non-Pair-Additive Intermolecular Potential Function to Fit Quantum-Mechanical Data on Water Molecule Interactions. J Chem Phys. 1977; 67:2338–2344.
150. Li J, Zhou Z, Sadus RJ. Role of Nonadditive Forces on the Structure and Properties of Liquid Water. J Chem Phys. 2007; 127:154509. [PubMed: 17949175]

151. Engkvist O, Forsberg N, Schutz M, Karlstrom G. A Comparison between the NEMO Intermolecular Water Potential and Ab Initio Quantum Chemical Calculations for the Water Trimer and Tetramer. Mol Phys. 1997; 90:277–287.

152. Holt A, Karlstrom G. Improvement of the NEMO Potential by Inclusion of Intramolecular Polarization. Int J Quantum Chem. 2009; 109:1255–1266.

153. Holt A, Karlstrom G. Inclusion of the Quadrupole Moment When Describing Polarization. The Effect of the Dipole-Quadrupole Polarizability. J Comput Chem. 2008; 29:2033–2038. [PubMed: 18432620]

154. Astrand PO, Wallqvist A, Karlstrom G. Intermolecular Interactions of Urea and Water. J Chim Phys Phys-Chim Biol. 1991; 88:2457–2464.

155. Astrand PO, Linse P, Karlstrom G. Molecular Dynamics Study of Water Adopting a Potential Function with Explicit Atomic Dipole-Moments and Anisotropic Polarizabilities. Chem Phys. 1995; 191:195–202.

156. Holt A, Bostrom J, Karlstrom G, Lindh R. A NEMO Potential that Includes the Dipole-Quadrupole and Quadrupole-Quadrupole Polarizability. J Comput Chem. 2010; 31:1583–1591. [PubMed: 20222056]

157. Carignano MA, Karlstrom G, Linse P. Polarizable Ions in Polarizable Water: A Molecular Dynamics Study. J Phys Chem B. 1997; 101:1142–1147.

158. Gao J, Truhlar DG, Wang Y, Mazack MJM, Loeffler P, Provorse MR, Rehak P. Explicit Polarization: A Quantum Mechanical Framework for Developing Next Generation Force Fields. Acc Chem Res. 2014; 47:2837–2845. [PubMed: 25098651]

159. Zhang P, Truhlar DG, Gao J. Fragment-Based Quantum Mechanical Methods for Periodic Systems with Ewald Summation and Mean Image Charge Convention for Long-Range Electrostatic Interactions. Phys Chem Chem Phys. 2012; 14:7821–7829. [PubMed: 22552612]

160. Han J, Mazack MJM, Zhang P, Truhlar DG, Gao J. Quantum Mechanical Force Field for Water with Explicit Electronic Polarization. J Chem Phys. 2013; 139:054503. [PubMed: 23927266]

161. Xie W, Orozco M, Truhlar DG, Gao J. X-Pol Potential: An Electronic Structure-Based Force Field for Molecular Dynamics Simulation of a Solvated Protein in Water. J Chem Theory Comput. 2009; 5:459–467. [PubMed: 20490369]

162. Handley CM, Hawe GI, Kell DB, Popelier PLA. Optimal Construction of a Fast and Accurate Polarisable Water Potential Based on Multipole Moments Trained by Machine Learning. Phys Chem Chem Phys. 2009; 11:6365–6376. [PubMed: 19809668]

163. Handley CM, Popelier PLA. Dynamically Polarizable Water Potential Based on Multipole Moments Trained by Machine Learning. J Chem Theory Comput. 2009; 5:1474–1489. [PubMed: 26609841]

164. Hawe GI, Popelier PLA. A Water Potential Based on Multipole Moments Trained by Machine Learning - Reducing Maximum Energy Errors. Can J Chem. 2010; 88:1104–1111.

165. Shaik MS, Liem SY, Popelier PLA. Properties of Liquid Water from a Systematic Refinement of a High-Rank Multipolar Electrostatic Potential. J Chem Phys. 2010; 132:174504. [PubMed: 20459171]

166. Torheyden M, Jansen G. A New Potential Energy Surface for the Water Dimer Obtained from Separate Fits of Ab Initio Electrostatic, Induction, Dispersion and Exchange Energy Contributions. Mol Phys. 2006; 104:2101–2138.

167. Singh UC, Kollman PA. A Water Dimer Potential Based on Ab Initio Calculations Using Morokuma Component Analyses. J Chem Phys. 1985; 83:4033–4040.

168. Nagata T, Fedorov DG, Kitaura K, Gordon MS. A Combined Effective Fragment Potential-Fragment Molecular Orbital Method. I. The Energy Expression and Initial Applications. J Chem Phys. 2009; 131:024101. [PubMed: 19603964]

169. Gordon MS, Freitag MA, Bandyopadhyay P, Jensen JH, Kairys V, Stevens WJ. The Effective Fragment Potential Method: A QM-Based MM Approach to Modeling Environmental Effects in Chemistry. J Phys Chem A. 2001; 105:293–307.

170. Netzloff HM, Gordon MS. The Effective Fragment Potential: Small Clusters and Radial Distribution Functions. J Chem Phys. 2004; 121:2711–2714. [PubMed: 15281872]

171. Kemp DA, Gordon MS. An Interpretation of the Enhancement of the Water Dipole Moment due to the Presence of Other Water Molecules. J Phys Chem A. 2008; 112:4885–4894. [PubMed: 18473449]

172. Mullin JM, Roskop LB, Pruitt SR, Collins MA, Gordon MS. Systematic Fragmentation Method and the Effective Fragment Potential: An Efficient Method for Capturing Molecular Energies. J Phys Chem A. 2009; 113:10040–10049. [PubMed: 19739681]

173. Honda K. An Effective Potential Function with Enhanced Charge-Transfer-Type Interaction for Hydrogen-Bonding Liquids. J Chem Phys. 2002; 117:3558–3569.

174. Gresh N. Computations of intermolecular interaction energies and nonadditivity effects. Comparisons between SIBFA and ab initio supermolecule calculations. Abstr Pap Am Chem S. 1998; 216:U706.

175. Piquemal JP, Gresh N, Giessner-Prettre C. Improved formulas for the calculation of the electrostatic contribution to the intermolecular interaction energy from multipolar expansion of the electronic distribution. J Phys Chem A. 2003; 107:10353–10359. [PubMed: 26313624]

176. Gresh N. Inter- and intramolecular interactions. Inception and refinements of the SIBFA, molecular mechanics (SMM) procedure, a separable, polarizable methodology grounded on ab initio SCF/MP2 computations. Examples of applications to molecular recognition problems. J Chim Phys Phys- Chim Biol. 1997; 94:1365–1416.

177. Gresh N, Cisneros GA, Darden TA, Piquemal JP. Anisotropic, polarizable molecular mechanics studies of inter- and intramoecular interactions and ligand-macromolecule complexes. A bottom-up strategy. J Chem Theory Comput. 2007; 3:1960–1986. [PubMed: 18978934]

178. Cisneros GA, Piquemal JP, Darden TA. Quantum mechanics/molecular mechanics electrostatic embedding with continuous and discrete functions. J Phys Chem B. 2006; 110:13682–13684. [PubMed: 16836309]

179. Piquemal JP, Cisneros GA, Reinhardt P, Gresh N, Darden TA. Towards a force field based on density fitting. J Chem Phys. 2006; 124:104101. [PubMed: 16542062]

180. Cisneros GA, Elking D, Piquemal JP, Darden TA. Numerical Fitting of Molecular Properties to Hermite Gaussians. J Phys Chem A. 2007; 111:12049–12056. [PubMed: 17973464]

181. Chaudret, R., Ulmer, S., van Severen, MC., Gresh, N., Parisel, O., Cisneros, GA., Darden, TA., Piquemal, JP. Progress Towards Accurate Molecular Modeling of Metal Complexes Using Polarizable Force Fields. In. In: Wei, DQ., Wang, XJ., editors. Theory and Applications of Computational Chemistry -2008. American Institute of Physics; 2009. p. 185-192.

182. Cisneros GA. Application of Gaussian Electrostatic Model (GEM) Distributed Multipoles in the AMOEBA Force Field. J Chem Theory Comput. 2012; 8:5072–5080. [PubMed: 26593198]

183. Chaudret R, Gresh N, Cisneros GA, Scemama A, Piquemal JP. Further Refinements of Next-Generation Force Fields -Nonempirical Localization of Off-Centered Points in Molecules. Can J Chem. 2013; 91:804–810.

184. Chaudret R, Gresh N, Narth C, Lagardere L, Darden TA, Cisneros GA, Piquemal JP. S/G-1: An Ab Initio Force-Field Blending Frozen Hermite Gaussian Densities and Distributed Multi-poles. Proof of Concept and First Applications to Metal Cations. J Phys Chem A. 2014; 118:7598–7612. [PubMed: 24878003]

185. Horn PR, Head-Gordon M. Alternative Definitions of the Frozen Energy in Energy Decomposition Analysis of Density Functional Theory Calculations. J Chem Phys. 2016; 144:084118. [PubMed: 26931692]

186. Temelso B, Archer KA, Shields GC. Benchmark Structures and Binding Energies of Small Water Clusters with Anharmonicity Corrections. J Phys Chem A. 2011; 115:12034–12046. [PubMed: 21910428]

187. Temelso B, Shields GC. The Role of Anharmonicity in Hydrogen-Bonded Systems: The Case of Water Clusters. J Chem Theory Comput. 2011; 7:2804–2817. [PubMed: 26605472]

188. Perez C, Muckle MT, Zaleski DP, Seifert NA, Temelso B, Shields GC, Kisiel Z, Pate BH. Structures of Cage, Prism, and Book Isomers of Water Hexamer from Broadband Rotational Spectroscopy. Science. 2012; 336:897–901. [PubMed: 22605772]

189. Duke RE, Starovoytov ON, Piquemal JP, Cisneros GA. GEM*: A Molecular Electronic Density-Based Force Field for Molecular Dynamics Simulations. J Chem Theory Comput. 2014; 10:1361–1365. [PubMed: 26580355]

190. Chaudret R, Gresh N, Parisel O, Piquemal JP. Many-Body Exchange-Repulsion in Polarizable Molecular Mechanics. I. Orbital-Based Approximations and Applications to Hydrated Metal Cation Complexes. J Comput Chem. 2011; 32:2949–2957. [PubMed: 21793002]

191. Babin V, Leforestier C, Paesani F. Development of a “First Principles” Water Potential with Flexible Monomers: Dimer Potential Energy Surface, VRT Spectrum, and Second Virial Coefficient. J Chem Theory Comput. 2013; 9:5395–5403. [PubMed: 26592277]

192. Burnham CJ, Xantheas SS. Development of Transferable Interaction Models for Water. I. Prominent Features of the Water Dimer Potential Energy Surface. J Chem Phys. 2002; 116:1479–1492.

193. Xantheas SS, Burnham CJ, Harrison RJ. Development of Transferable Interaction Models for Water. II. Accurate Energetics of the First Few Water Clusters from First Principles. J Chem Phys. 2002; 116:1493–1499.

194. Burnham CJ, Xantheas SS. Development of Transferable Interaction Models for Water. III. Reparametrization of an All-Atom Polarizable Rigid Model (TTM2-R) from First Principles. J Chem Phys. 2002; 116:1500–1510.

195. Burnham CJ, Xantheas SS. Development of Transferable Interaction Models for Water. IV. A Flexible, All-Atom Polarizable Potential (TTM2-F) Based on Geometry Dependent Charges Derived from an Ab Initio Monomer Dipole Moment Surface. J Chem Phys. 2002; 116:5115–5124.

196. Fanourgakis GS, Xantheas SS. The Flexible, Polarizable, Thole-Type Interaction Potential for Water (TTM2-F) Revisited. J Phys Chem A. 2006; 110:4100–4106. [PubMed: 16539435]

197. Partridge H, Schwenke DW. The Determination of an Accurate Isotope Dependent Potential Energy Surface for Water from Extensive Ab Initio Calculations and Experimental Data. J Chem Phys. 1997; 106:4618–4639.

198. Thole BT. Molecular Polarizabilities Calculated with a Modified Dipole Interaction. Chem Phys. 1981; 59:341–350.

199. Fanourgakis GS, Schenter GK, Xantheas SS. A Quantitative Account of Quantum Effects in Liquid Water. J Chem Phys. 2006; 125:141102. [PubMed: 17042571]

200. Fanourgakis GS, Xantheas SS. The Bend Angle of Water in Ice Ih and Liquid Water: The Significance of Implementing the Nonlinear Monomer dipole moment surface in classical interaction potentials. J Chem Phys. 2006; 124:174504. [PubMed: 16689580]

201. Paesani F, Iuchi S, Voth GA. Quantum Effects in Liquid Water from an Ab Initio-Based Polarizable Force Field. J Chem Phys. 2007; 127:074506. [PubMed: 17718619]

202. Paesani F, Yoo S, Bakker HJ, Xantheas SS. Nuclear Quantum Effects in the Reorientation of Water. J Phys Chem Lett. 2010; 1:2316–2321.

203. Paesani F, Xantheas SS, Voth GA. Infrared Spectroscopy and Hydrogen-Bond Dynamics of Liquid Water from Centroid Molecular Dynamics with an Ab Initio-Based Force Field. J Phys Chem B. 2009; 113:13118–13130. [PubMed: 19722542]

204. Paesani F. Temperature-Dependent Infrared Spectroscopy of Water from a First-Principles Approach. J Phys Chem A. 2011; 115:6861–6871. [PubMed: 21247204]

205. Paesani F. Hydrogen-Bond Dynamics in Heavy Water Studied with Quantum Dynamical Simulations. Phys Chem Chem Phys. 2011; 13:19865–19875. [PubMed: 21892511]

206. Kumar R, Wang FF, Jenness GR, Jordan KD. A Second Generation Distributed Point Polarizable Water Model. J Chem Phys. 2010; 132:014309. [PubMed: 20078163]

207. Mankoo PK, Keyes T. POLIR: Polarizable, Flexible, Transferable Water Potential Optimized for IR Spectroscopy. J Chem Phys. 2008; 129:034504. [PubMed: 18647028]

208. Hasegawa T, Tanimura Y. A Polarizable Water Model for Intramolecular and Intermolecular Vibrational Spectroscopies. J Phys Chem B. 2011; 115:5545–5553. [PubMed: 21486049]

209. Millot C, Stone AJ. Towards and Accurate Intermolecular Potential for Water. Mol Phys. 1992; 77:439–462.

210. Millot C, Soetens JC, Martins Costa MTC, Hodges MP, Stone AJ. Revised Anisotropic Site Potentials for the Water Dimer and Calculated Properties. J Phys Chem A. 1998; 102:754–770.
211. Goldman N, Fellers RS, Brown MG, Braly LB, Keoshian CJ, Leforestier C, Saykally RJ. Spectroscopic Determination of the Water Dimer Intermolecular Potential-Energy Surface. J Chem Phys. 2002; 116:10148–10163.
212. Goldman N, Leforestier C, Saykally RJ. A 'First Principles' Potential Energy Surface for Liquid Water from VRT Spectroscopy of Water Clusters. Philos Trans R Soc, A. 2005; 363:493–508.
213. Wikfeldt KT, Batista ER, Vila FD, Jonsson H. A Transferable H_2O Interaction Potential Based on a Single Center Multipole Expansion: SCME. Phys Chem Chem Phys. 2013; 15:16542–16556. [PubMed: 23949215]
214. Batista ER, Xantheas SS, Jonsson H. Molecular Multipole Moments of Water Molecules in Ice Ih. J Chem Phys. 1998; 109:4546–4551.
215. Batista ER, Xantheas SS, Jonsson H. Electric Fields in Ice and Near Water Clusters. J Chem Phys. 2000; 112:3285–3292.
216. Tribello GA, Slater B. Proton Ordering Energetics in Ice Phases. Chem Phys Lett. 2006; 425:246–250.
217. Medders GR, Götz AW, Morales MA, Bajaj P, Paesani F. On the Representation of Many-Body Interactions in Water. J Chem Phys. 2015; 143:104102. [PubMed: 26374013]
218. Bates DM, Tschumper GS. CCSD(T) Complete Basis Set Limit Relative Energies for Low-Lying Water Hexamer Structures. J Phys Chem A. 2009; 113:3555–3559. [PubMed: 19354314]
219. Paesani F, Voth GA. The Properties of Water: Insights from Quantum Simulations. J Phys Chem B. 2009; 113:5702–5719. [PubMed: 19385690]
220. Stone AJ. Electrostatic Damping Functions and the Penetration Energy. J Phys Chem A. 2011; 115:7017–7027. [PubMed: 21619003]
221. Cui J, Liu HB, Jordan KD. Theoretical Characterization of the $(H_2O)_{21}$ Cluster: Application of an N-Body Decomposition Procedure. J Phys Chem B. 2006; 110:18872–18878. [PubMed: 16986878]
222. Khaliullin RZ, Cobar EA, Lochan RC, Bell AT, Head-Gordon M. Unravelling the Origin of Intermolecular Interactions Using Absolutely Localized Molecular Orbitals. J Phys Chem A. 2007; 111:8753–8765. [PubMed: 17655284]
223. Niesar U, Corongiu G, Huang MJ, Dupuis M, Clementi E. Preliminary Observations on a New Water-Water Potential. Int J Quantum Chem. 1989; 36:421–443.
224. Niesar U, Corongiu G, Clementi E, Kneller GR, Bhattacharya DK. Molecular Dynamics Simulations of Liquid Water Using the NCC Ab Initio Potential. J Phys Chem. 1990; 94:7949–7956.
225. Groenenboom GC, Mas EM, Bukowski R, Szalewicz K, Wormer PES, van der Avoird A. Water Pair and Three-Body Potential of Spectroscopic Quality from Ab Initio Calculations. Phys Rev Lett. 2000; 84:4072–4075. [PubMed: 10990613]
226. Mas EM, Bukowski R, Szalewicz K. Ab Initio Three-Body Interactions for Water. I. Potential and Structure of Water Trimer. J Chem Phys. 2003; 118:4386–4403.
227. Mas EM, Bukowski R, Szalewicz K. Ab Initio Three-Body Interactions for Water. II. Effects on Structure and Energetics of Liquid. J Chem Phys. 2003; 118:4404–4413.
228. Bukowski R, Szalewicz K, Groenenboom GC, van der Avoird A. Predictions of the Properties of Water from First Principles. Science. 2007; 315:1249–1252. [PubMed: 17332406]
229. Bukowski R, Szalewicz K, Groenenboom GC, van der Avoird A. Polarizable Interaction Potential for Water from Coupled Cluster Calculations. I. Analysis of Dimer Potential Energy Surface. J Chem Phys. 2008; 128:094313. [PubMed: 18331099]
230. Bukowski R, Szalewicz K, Groenenboom GC, van der Avoird A. Polarizable Interaction Potential for Water from Coupled Cluster Calculations. II. Applications to Dimer Spectra, Virial Coefficients, and Simulations of Liquid Water. J Chem Phys. 2008; 128:094314. [PubMed: 18331100]
231. Cencek W, Szalewicz K, Leforestier C, van Harrevelt R, van der Avoird A. An Accurate Analytic Representation of the Water Pair Potential. Phys Chem Chem Phys. 2008; 10:4716–4731. [PubMed: 18688514]

232. Gora U, Cencek W, Podeszwa R, van der Avoird A, Szalewicz K. Predictions for Water Clusters from a First-Principles Two- and Three-Body Force Field. J Chem Phys. 2014; 140:194101. [PubMed: 24852524]
233. Szalewicz K, Leforestier C, van der Avoird A. Towards the Complete Understanding of Water by a First-Principles Computational Approach. Chem Phys Lett. 2009; 482:1–14.
234. Jankowski P, Murdachaew G, Bukowski R, Akin-Ojo O, Leforestier C, Szalewicz K. Ab Initio Water Pair Potential with Flexible Monomers. J Phys Chem A. 2015; 119:2940–2964. [PubMed: 25687650]
235. Huang XC, Braams BJ, Bowman JM. Ab Initio Potential Energy and Dipole Moment Surfaces of $(H_2O)_2$. J Phys Chem A. 2006; 110:445–451. [PubMed: 16405316]
236. Wang YM, Bowman JM. Ab Initio Potential and Dipole Moment Surfaces for Water. II. Local-Monomer Calculations of the Infrared Spectra of Water Clusters. J Chem Phys. 2011; 134:154510. [PubMed: 21513398]
237. Wang YM, Shepler BC, Braams BJ, Bowman JM. Full-Dimensional, Ab Initio Potential Energy and Dipole Moment Surfaces for Water. J Chem Phys. 2009; 131:054511. [PubMed: 19673578]
238. Wang YM, Bowman JM. Towards an Ab Initio Flexible Potential for Water, and Post-Harmonic Quantum Vibrational Analysis of Water Clusters. Chem Phys Lett. 2010; 491:1–10.
239. Braams BJ, Bowman JM. Permutationally Invariant Potential Energy Surfaces in High Dimensionality. Int Rev Phys Chem. 2009; 28:577–606.
240. Ch'ng LC, Samanta AK, Czako G, Bowman JM, Reisler H. Experimental and Theoretical Investigations of Energy Transfer and Hydrogen-Bond Breaking in the Water Dimer. J Am Chem Soc. 2012; 134:15430–15435. [PubMed: 22917255]
241. Ch'ng LC, Samanta AK, Wang YM, Bowman JM, Reisler H. Experimental and Theoretical Investigations of the Dissociation Energy (D_0) and Dynamics of the Water Trimer, $(H_2O)_3$. J Phys Chem A. 2013; 117:7207–7216. [PubMed: 23536966]
242. Wang YM, Babin V, Bowman JM, Paesani F. The Water Hexamer: Cage, Prism, or Both. Full Dimensional Quantum Simulations Say Both. J Am Chem Soc. 2012; 134:11116–11119. [PubMed: 22731508]
243. Wang YM, Bowman JM. IR Spectra of the Water Hexamer: Theory, with Inclusion of the Monomer Bend Overtone, and Experiment Are in Agreement. J Phys Chem Lett. 2013; 4:1104–1108. [PubMed: 26282028]
244. Liu HC, Wang YM, Bowman JM. Local-Monomer Calculations of the Intramolecular IR Spectra of the Cage and Prism Isomers of $HOD(D_2O)_5$ and HOD and D_2O Ice lh. J Phys Chem B. 2014; 118:14124–14131. [PubMed: 25010120]
245. Liu HC, Wang YM, Bowman JM. Quantum Calculations of the IR Spectrum of Liquid Water Using Ab Initio and Model Potential and Dipole Moment Surfaces and Comparison with Experiment. J Chem Phys. 2015; 142:194502. [PubMed: 26001464]
246. Bowman JM, Wang YM, Liu HC, Mancini JS. Ab Initio Quantum Approaches to the IR Spectroscopy of Water and Hydrates. J Phys Chem Lett. 2015; 6:366–373. [PubMed: 26261949]
247. Liu HC, Wang YM, Bowman JM. Vibrational Analysis of an Ice Ih Model from 0 to 4000 cm^{-1} Using the Ab Initio WHBB Potential Energy Surface. J Phys Chem B. 2013; 117:10046–10052. [PubMed: 23924359]
248. Babin V, Paesani F. The Curious Case of the Water Hexamer: Cage vs. Prism. Chem Phys Lett. 2013; 580:1–8.
249. Medders GR, Babin V, Paesani F. Development of a "First-Principles" Water Potential with Flexible Monomers. III. Liquid Phase Properties. J Chem Theory Comput. 2014; 10:2906–2910. [PubMed: 26588266]
250. Howard JC, Tschumper GS. Benchmark Structures and Harmonic Vibrational Frequencies Near the CCSD(T) Complete Basis Set Limit for Small Water Clusters: $(H_2O)_{n=2, 3, 4, 5, 6}$. J Chem Theory Comput. 2015; 11:2126–2136. [PubMed: 26574415]
251. Morales MA, Gergely JR, McMinis J, McMahon JM, Kim J, Ceperley DM. Quantum Monte Carlo Benchmark of Exchange-Correlation Functionals for Bulk Water. J Chem Theory Comput. 2014; 10:2355–2362. [PubMed: 26580755]

252. Wiener, N. Extrapolation, Interpolation and Smoothing of Stationary Time Series. MIT Press; Cambridge: 1949.

253. Matheron G. The Intrinsic Random Functions and their Applications. Adv Appl Probab. 1973; 5:439–468.

254. Bartók AP, Payne MC, Kondor R, Csanyi G. Gaussian Approximation Potentials: The Accuracy of Quantum Mechanics, Without the Electrons. Phys Rev Lett. 2010; 104:136403. [PubMed: 20481899]

255. Bartók AP, Csanyi G. Gaussian Approximation Potentials: A Brief Tutorial Introduction. Int J Quantum Chem. 2015; 115:1051–1057.

256. Bartok AP, Gillan MJ, Manby FR, Csanyi G. Machine-Learning Approach for One- and Two-Body Corrections to Density Functional Theory: Applications to Molecular and Condensed Water. Phys Rev B: Condens Matter Mater Phys. 2013; 88:054104.

257. Grimme S, Ehrlich S, Goerigk L. Effect of the Damping Function in Dispersion Corrected Density Functional Theory. J Comput Chem. 2011; 32:1456–1465. [PubMed: 21370243]

258. Frisch, MJ., Trucks, GW., Schlegel, HB., Scuseria, GE., Robb, MA., Cheeseman, JR., Scalmani, G., Barone, V., Mennucci, B., Petersson, GA., Nakatsuji, H., Caricato, M., Li, X., Hratchian, HP., Izmaylov, AF., Bloino, J., Zheng, G., Sonnenberg, JL., Hada, M., Ehara, M., Toyota, K., Fukuda, R., Hasegawa, J., Ishida, M., Nakajima, T., Honda, Y., Kitao, O., Nakai, H., Vreven, T., Montgomery, JA., Jr, Peralta, JE., Ogliaro, F., Bearpark, MJ., Heyd, J., Brothers, EN., Kudin, KN., Staroverov, VN., Kobayashi, R., Normand, J., Raghavachari, K., Rendell, AP., Burant, JC., Iyengar, SS., Tomasi, J., Cossi, M., Rega, N., Millam, NJ., Klene, M., Knox, JE., Cross, JB., Bakken, V., Adamo, C., Jaramillo, J., Gomperts, R., Stratmann, RE., Yazyev, O., Austin, AJ., Cammi, R., Pomelli, C., Ochterski, JW., Martin, RL., Morokuma, K., Zakrzewski, VG., Voth, GA., Salvador, P., Dannenberg, JJ., Dapprich, S., Daniels, AD., Farkas, Ö., Foresman, JB., Ortiz, JV., Cioslowski, J., Fox, DJ. Gaussian 09. Gaussian, Inc; Wallingford, CT: 2009.

259. Gillan MJ, Alfè D, Michaelides A. Perspective: How Good Is DFT for Water? J Chem Phys. 2016; 144:130901. [PubMed: 27059554]

260. Medders GR, Paesani F. Many-Body Convergence of the Electrostatic Properties of Water. J Chem Theory Comput. 2013; 9:4844–4852. [PubMed: 26583403]

261. Medders GR, Paesani F. Infrared and Raman Spectroscopy of Liquid Water Through “First-Principles” Many-Body Molecular Dynamics. J Chem Theory Comput. 2015; 11:1145–1154. [PubMed: 26579763]

262. Medders GR, Paesani F. On the Interplay of the Potential Energy and Dipole Moment Surfaces in Controlling the Infrared Activity of Liquid Water. J Chem Phys. 2015; 142:212411. [PubMed: 26049431]

263. Leverentz HR, Qi HW, Truhlar DG. Assessing the Accuracy of Density Functional and Semiempirical Wave Function Methods for Water Nanoparticles: Comparing Binding and Relative Energies of $(H_2O)_{16}$ and $(H_2O)_{17}$ to CCSD(T) Results. J Chem Theory Comput. 2013; 9:995–1006. [PubMed: 26588742]

264. Friedrich J, Yu HY, Leverentz HR, Bai P, Siepmann JI, Truhlar DG. Water 26-mers Drawn from Bulk Simulations: Benchmark Binding Energies for Unprecedentedly Large Water Clusters and Assessment of the Electrostatically Embedded Three-Body and Pairwise Additive Approximations. J Phys Chem Lett. 2014; 5:666–670. [PubMed: 26270834]

265. Qi HW, Leverentz HR, Truhlar DG. Water 16-mers and Hexamers: Assessment of the Three-Body and Electrostatically Embedded Many-Body Approximations of the Correlation Energy or the Nonlocal Energy As Ways to Include Cooperative Effects. J Phys Chem A. 2013; 117:4486–4499. [PubMed: 23627665]

266. Miliordos E, Aprà E, Xantheas SS. Optimal Geometries and Harmonic Vibrational Frequencies of the Global Minima of Water Clusters $(H_2O)_n$, n = 2–6: and Several Hexamer Local Minima at the CCSD(T) Level of Theory. J Chem Phys. 2013; 139:114302. [PubMed: 24070285]

267. Warshel A, Kato M, Pisliakov AV. Polarizable Force Fields: History, Test Cases, and Prospects. J Chem Theory Comput. 2007; 3:2034–2045. [PubMed: 26636199]

268. Laury ML, Wang LP, Pande VS, Head-Gordon T, Ponder JW. Revised Parameters for the AMOEBA Polarizable Atomic Multipole Water Model. J Phys Chem B. 2015; 119:9423–9437. [PubMed: 25683601]
269. Steinbach PJ, Brooks BR. New Spherical-Cutoff Methods for Long-Range Forces in Macromolecular Simulation. J Comput Chem. 1994; 15:667–683.
270. Paesani Group. mbpol_openmm_plugin. 2015. http://paesanigroup.ucsd.edu/software/mbpol.html
271. Ceriotti M, Parrinello M, Markland TE, Manolopoulos DE. Efficient Stochastic Thermostatting of Path Integral Molecular Dynamics. J Chem Phys. 2010; 133:124104. [PubMed: 20886921]
272. Ceriotti M, Bussi G, Parrinello M. Colored-Noise Thermostats á la Carte. J Chem Theory Comput. 2010; 6:1170–1180.
273. Markland TE, Manolopoulos DE. An Efficient Ring Polymer Contraction Scheme for Imaginary Time Path Integral Simulations. J Chem Phys. 2008; 129:024105. [PubMed: 18624514]
274. Rheinecker JL, Bowman JM. The Calculated Infrared Spectrum of Cl^-H_2O Using a Full Dimensional Ab Initio Potential Surface and Dipole Moment Surface. J Chem Phys. 2006; 124:131102. [PubMed: 16613440]
275. Rheinecker J, Bowman JM. The Calculated Infrared Spectrum of Cl^-H_2O Using a New Full Dimensional Ab Initio Potential Surface and Dipole Moment Surface. J Chem Phys. 2006; 125:133206. [PubMed: 17029453]
276. Kamarchik E, Bowman JM. Coupling of Low- and High-Frequency Vibrational Modes: Broadening in the Infrared Spectrum of $F^-(H_2O)_2$. J Phys Chem Lett. 2013; 4:2964–2969.
277. Kamarchik E, Toffoli D, Christiansen O, Bowman JM. Ab Initio Potential Energy and Dipole Moment Surfaces of the F-(H_2O) Complex. Spectrochim Acta, Part A. 2014; 119:59–62.
278. Wolke CT, Menges FS, Totsch N, Gorlova O, Fournier JA, Weddle GH, Johnson MA, Heine N, Esser TK, Knorke H, Asmis KR, McCoy AB, Arismendi-Arrieta DJ, Prosmiti R, Paesani F. Thermodynamics of Water Dimer Dissociation in the Primary Hydration Shell of the Iodide Ion with Temperature-Dependent Vibrational Predissociation Spectroscopy. J Phys Chem A. 2015; 119:1859–1866. [PubMed: 25647222]
279. Arismendi-Arrieta DJ, Riera M, Bajaj P, Prosmiti R, Paesani F. i-TTM Model for Ab Initio-Based Ion-Water Interaction Potentials. I. Halide-Water Potential Energy Functions. J Phys Chem B. 2016; 120:1822–1832. [PubMed: 26560189]
280. Bajaj P, Götz AW, Paesani F. Toward Chemical Accuracy in the Description of Ion-Water Interactions Through Many-Body Representations. I. Halide-Water Dimer Potential Energy Surfaces. J Chem Theory Comput. 2016; doi: 10.1021/acs.jctc.6b00302
281. Riera M, Götz AW. i-TTM Model for Ab Initio-Based Ion-Water Interaction Potentials. II. Alkali Metal Ion–Water Potential Energy Functions. Phys Chem Chem Phys. 2016 under review.
282. Pinski P, Csanyi G. Reactive Many-Body Expansion for a Protonated Water Cluster. J Chem Theory Comput. 2014; 10:68–75. [PubMed: 26579892]
283. Kerdcharoen T, Liedl KR, Rode BM. A QM/MM Simulation Method Applied to the Solution of Li^+ in Liquid Ammonia. Chem Phys. 1996; 211:313–323.
284. Rode BM, Hofer TS, Randolf BR, Schwenk CF, Xenides D, Vchirawongkwin V. Ab Initio Quantum Mechanical Charge Field (QMCF) Molecular Dynamics: A QM/MM-MD Procedure for Accurate Simulations of Ions and Complexes. Theor Chem Acc. 2006; 115:77–85.
285. Heyden A, Lin H, Truhlar DG. Adaptive Partitioning in Combined Quantum Mechanical and Molecular Mechanical Calculations of Potential Energy Functions for Multiscale Simulations. J Phys Chem B. 2007; 111:2231–2241. [PubMed: 17288477]
286. Heyden A, Truhlar DG. Conservative Algorithm for an Adaptive Change of Resolution in Mixed Atomistic/Coarse-Grained Multiscale Simulations. J Chem Theory Comput. 2008; 4:217–221. [PubMed: 26620653]
287. Bulo RE, Ensing B, Sikkema J, Visscher L. Toward a Practical Method for Adaptive QM/MM Simulations. J Chem Theory Comput. 2009; 5:2212–2221. [PubMed: 26616607]
288. Park K, Gotz AW, Walker RC, Paesani F. Application of Adaptive QM/MM Methods to Molecular Dynamics Simulations of Aqueous Systems. J Chem Theory Comput. 2012; 8:2868–2877. [PubMed: 26592126]

289. Rowley CN, Roux B. The Solvation Structure of Na^+ and K^+ in Liquid Water Determined from High Level Ab Initio Molecular Dynamics Simulations. J Chem Theory Comput. 2012; 8:3526–3535. [PubMed: 26593000]

290. Bulo RE, Michel C, Fleurat-Lessard P, Sautet P. Multiscale Modeling of Chemistry in Water: Are We There Yet? J Chem Theory Comput. 2013; 9:5567–5577. [PubMed: 26592290]

291. Mones L, Jones A, Gotz AW, Laino T, Walker RC, Leimkuhler B, Csanyi G, Bernstein N. The Adaptive Buffered Force QM/MM Method in the CP2K and AMBER Software Packages. J Comput Chem. 2015; 36:633–648. [PubMed: 25649827]

292. Wang L, Ceriotti M, Markland TE. Quantum Fluctuations and Isotope Effects in Ab Initio Descriptions of Water. J Chem Phys. 2014; 141:104502. [PubMed: 25217932]

293. DiStasio RA, Santra B, Li ZF, Wu XF, Car R. The Individual and Collective Effects of Exact Exchange and Dispersion Interactions on the Ab Initio Structure of Liquid Water. J Chem Phys. 2014; 141:084502. [PubMed: 25173016]

294. Laury ML, Wang LP, Pande VS, Head-Gordon T, Ponder JW. Revised Parameters for the AMOEBA Polarizable Atomic Multipole Water Model. J Phys Chem B. 2015; 119:9423–9437. [PubMed: 25683601]

295. Leforestier C. Infrared Shifts of the Water Dimer from the Fully Flexible Ab Initio HBB2 Potential. Philos Trans R Soc, A. 2012; 370:2675–2690.

296. Leforestier C, Szalewicz K, van der Avoird A. Spectra of Water Dimer from a New Ab Initio Potential with Flexible Monomers. J Chem Phys. 2012; 137:014305. [PubMed: 22779646]

297. Fraser GT. $(H_2O)_2$ - Spectroscopy Structure and Dynamics. Int Rev Phys Chem. 1991; 10:189–206.

298. Zwart E, Termeulen JJ, Meerts WL, Coudert LH. The Submillimiter Rotation Tunneling Spectrum of the Water Dimer. J Mol Spectrosc. 1991; 147:27–39.

299. Braly LB, Liu K, Brown MG, Keutsch FN, Fellers RS, Saykally RJ. Terahertz Laser Spectroscopy of the Water Dimer Intermolecular Vibrations. II. $(H_2O)_2$. J Chem Phys. 2000; 112:10314–10326.

300. Keutsch FN, Braly LB, Brown MG, Harker HA, Petersen PB, Leforestier C, Saykally RJ. Water Dimer Hydrogen Bond Stretch, Donor Torsion Overtone, and “In-Plane Bend” Vibrations. J Chem Phys. 2003; 119:8927–8937.

301. Keutsch FN, Goldman N, Harker HA, Leforestier C, Saykally RJ. Complete Characterization of the Water Dimer Vibrational Ground State and Testing the VRT(ASP-W)III, SAPT-5st, and VRT(MCY-5f) surfaces. Mol Phys. 2003; 101:3477–3492.

302. Howard JC, Gray JL, Hardwick AJ, Nguyen LT, Tschumper GS. Getting Down to the Fundamentals of Hydrogen Bonding: Anharmonic Vibrational Frequencies of $(HF)_2$ and $(H_2O)_2$ from Ab Initio Electronic Structure Computations. J Chem Theory Comput. 2014; 10:5426–5435. [PubMed: 26583226]

303. Bakker HJ, Skinner JL. Vibrational Spectroscopy as a Probe of Structure and Dynamics in Liquid Water. Chem Rev. 2010; 110:1498–1517. [PubMed: 19916491]

304. Kell GS. Density, Thermal Expansivity, and Compressibility of Liquid Water from 0° to 150 °C-Correlations and Tables for Atmospheric-Pressure and Saturation Reviewed and Expressed on 1968 Temperature Scale. J Chem Eng Data. 1975; 20:97–105.

Biographies

G. Andrés Cisneros received a B.Sc. in Chemistry from the National Autonomous University of Mexico (UNAM) and a Ph.D. in Chemistry from Duke University. Afterward, he worked as an intramural postdoctoral fellow in the National Institute of Environmental Health Sciences/NIH. He is currently an Associate Professor in the Department of Chemistry at Wayne State University. His research interests include development and application of accurate methods for chemical/biochemical simulations with emphasis on

force field and QM/MM development, and the study of DNA replication/repair systems and ionic liquids.

Kjartan Thor Wikfeldt obtained his Ph.D. degree from the group of Prof. Lars G.M. Pettersson at Stockholm University, Sweden, in 2011, and subsequently held postdoctoral research positions in Prof. Angelos Michaelides' group at University College London, UK, and in Prof. Hannes Jónsson's group at the University of Iceland. Currently, he has joint research associate positions at the University of Iceland and Stockholm University where he focuses on computational research related to liquid water, crystalline and amorphous ice, and chemical reactions on ice surfaces in interstellar molecular clouds.

Lars Ojamäe received his Ph.D. in inorganic chemistry from Uppsala University in 1993, worked as a postdoc at the Ohio State University and the University of Turin, as assistant professor at Stockholm University and associate professor and then full professor at Linköping University, where he currently heads the physical chemistry subdivision. His research activities focus on computational-chemistry modeling of hydrogen-bonded systems such as ice and clathrates, as well as chemical reactions at surfaces of relevance for catalysis, solar cells, and nanoparticles.

Jibao Lu received his Ph.D in condensed matter physics in Prof. Ying Dai's group at Shandong University (China) in 2012. Since then, he has worked as a postdoc at The University of Utah. His research interests involve the development of coarse-grained models, computational study of water-like tetrahedral liquids, anion-exchange membranes for alkaline fuel cells, and photocatalytic and magnetic semiconductors.

Yao Xu earned his B.Sc. in Applied Chemistry from Beijing University of Chemical Technology (China) in 2006 and his Ph.D. in Chemical Physics from the University of Nevada, Reno under the supervision of Prof. David M. Leitner in 2013. He currently is a postdoctoral researcher in the group of Prof. Martina Havenith at Ruhr University Bochum, Germany. He is interested in connecting solvation dynamics with biomolecular functions by molecular simulation and laser spectroscopy.

Hedieh Torabifard received her B.Sc. in Chemistry from Shahid Beheshti University (Iran) in 2008 and her M.Sc. in Physical Organic Chemistry in 2011 from Sharif University of Technology (Iran). She is currently a Ph.D. student in the group of Prof. G. Andrés Cisneros at Wayne State University. Her research interests involve the development of multipolar–polarizable force fields for condensed systems and QM/MM studies of biochemical systems.

Albert P. Bartók was awarded his Ph.D. in 2010 after studying in Cambridge under the supervision of Prof. Mike Payne and Prof. Gábor Csányi. He held a Junior Research Fellowship in Magdalene College until 2013 and has been a Leverhulme Early Career Fellow since then. His main research interest is fitting accurate potentials using probabilistic machine learning techniques.

Gábor Csányi obtained a B.A. in Mathematics from the University of Cambridge in 1994 and a Ph.D. in Physics at the Massachusetts Institute of Technology in 2001. He is on the

faculty of the Engineering Laboratory at the University of Cambridge, and his research focuses on developing new methods and algorithms for molecular simulation.

Valeria Molinero received her Ph.D. in Physical Chemistry from the University of Buenos Aires in 1999, worked as associate scientist at Caltech and Arizona State University, and joined the faculty at The University of Utah in 2006, where she is Professor of Chemistry and Director of the Henry Eyring Center for Theoretical Chemistry. Molinero is interested in the interplay between microscopic structure, dynamics, and phase transformations in materials. The modeling of water, its anomalies and phase transitions has been a focus in her research in the last years.

Francesco Paesani received his Ph.D. in Theoretical Physical Chemistry from the University of Rome "'La Sapienza"' (Italy) in 2000. He was a postdoctoral fellow at the University of California, Berkeley, working with Professor Birgitta Whaley on the spectroscopy and superfluid behavior of helium droplets at low temperature. Subsequently, he was a postdoctoral researcher in the group of Professor Gregory Voth at the University of Utah working on the development of new methodologies to model quantum dynamics in the condensed phase. In 2009, he joined the faculty of the University of California, San Diego, where he is currently an Associate Professor in the Department of Chemistry and Biochemistry. In 2016, he was awarded the ACS Early Career Award in Theoretical Chemistry. Research in his group focuses on the development, implementation, and application of new theoretical and computational methodologies at the intersection between chemistry, physics, and computer science for molecular-level simulations of fundamental processes from the gas to the condensed phase.

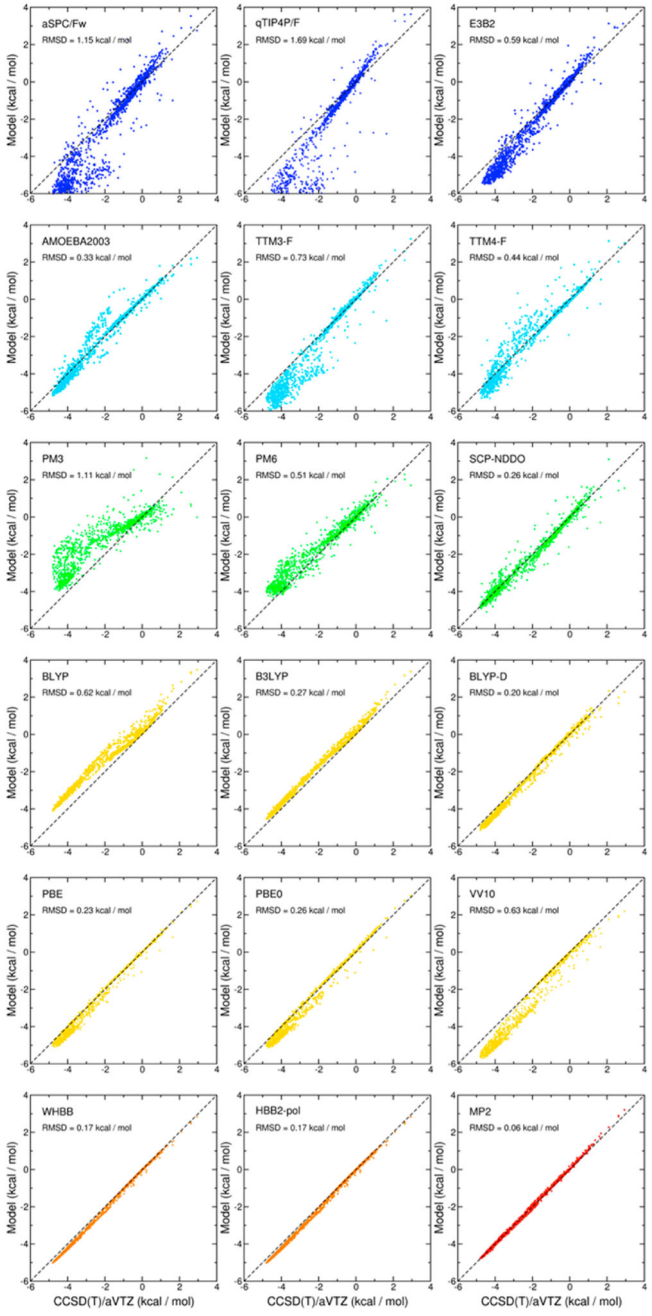

Figure 1.

Correlation plots for 2B interaction energies. Plotted on the *x* axes are the BSSE-corrected CCSD(T) reference energies calculated with the aug-cc-pVTZ (aVTZ) basis set for ~1400 water dimers. On the *y* axes are the corresponding energies calculated with the different water PESs. Color scheme: empirical models = blue, polarizable models = light blue, semiempirical models = green, DFT models = yellow, explicit many-body models = orange, and MP2 = red. All data were taken from ref 32.

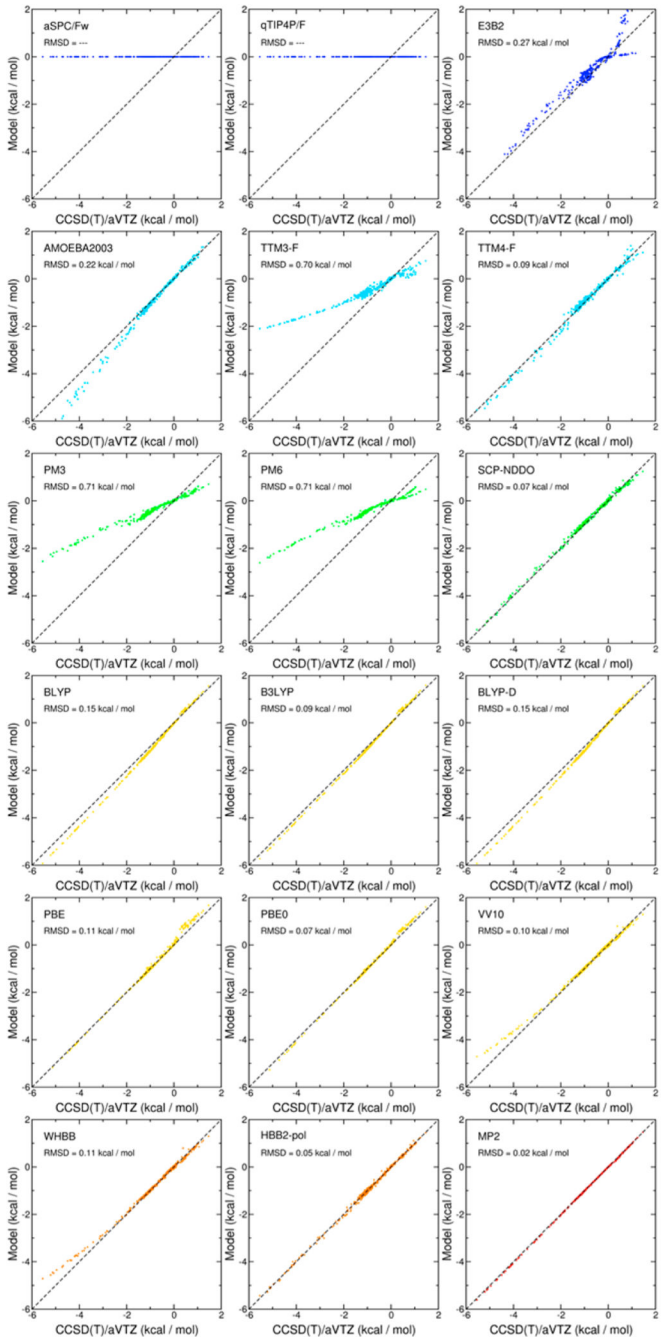

Figure 2.

Correlation plots for 3B interaction energies. Plotted on the *x* axes are the BSSE-corrected CCSD(T) reference energies calculated with the aug-cc-pVTZ (aVTZ) basis set for ~500 water trimers. On the *y* axes are the corresponding energies calculated with the different water PESs. Color scheme: empirical models = blue, polarizable models = light blue, semiempirical models = green, DFT models = yellow, explicit many-body models = orange, and MP2 = red. All data were taken from ref 32.

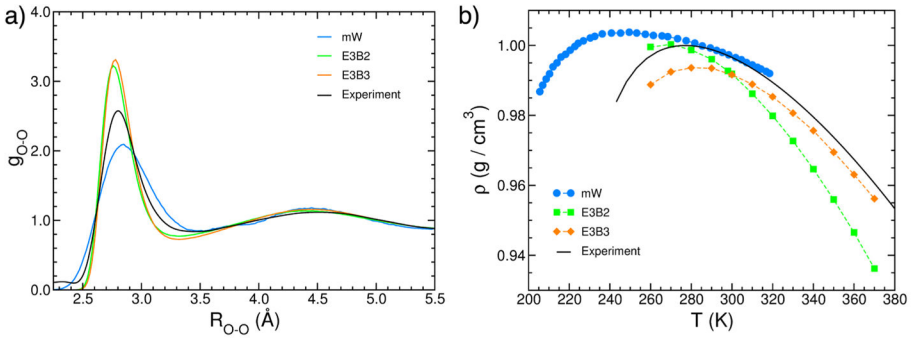

Figure 3.

(a) Comparison between oxygen–oxygen radial distribution functions of liquid water at ambient conditions derived from X-ray diffraction measurements (black)[108] and calculated from molecular dynamics simulations performed with the coarse-grained mW model (blue)[100] and the empirical E3B models (green and orange).[38,107] (b) Comparison between the experimental and calculated temperature dependence of the density of liquid water at ambient pressure. The experimental values (black) are from ref 304.

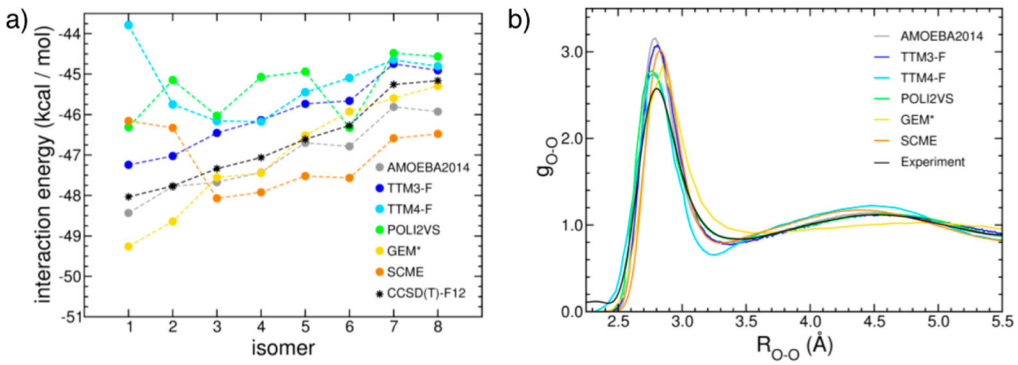

Figure 4.

(a) Interaction energies of the water hexamer isomers calculated with six polarizable force fields using the MP2 optimized geometries of ref 218 shown in Figure 5. Also shown as a reference are the corresponding values obtained at the CCSD(T)-F12 level in the complete basis set limit.[217] (b) Comparison between the oxygen–oxygen radial distribution functions of liquid water at ambient conditions derived from X-ray diffraction measurements (black)[108] and calculated from molecular dynamics simulations performed with six polarizable force fields. The AMOEBA2014 and POLI2VS results are from refs 268 and 208, respectively.

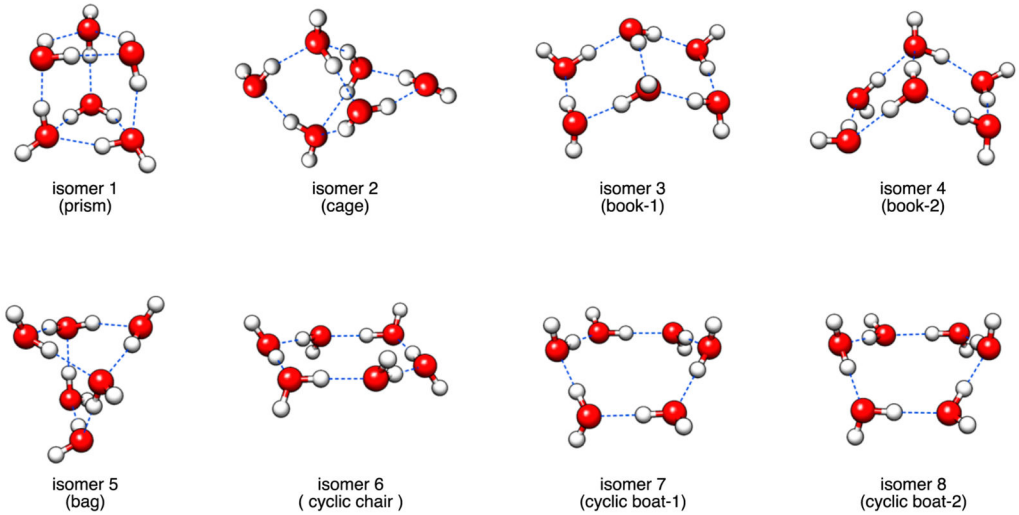

Figure 5.
Low-energy isomers of the water hexamer.

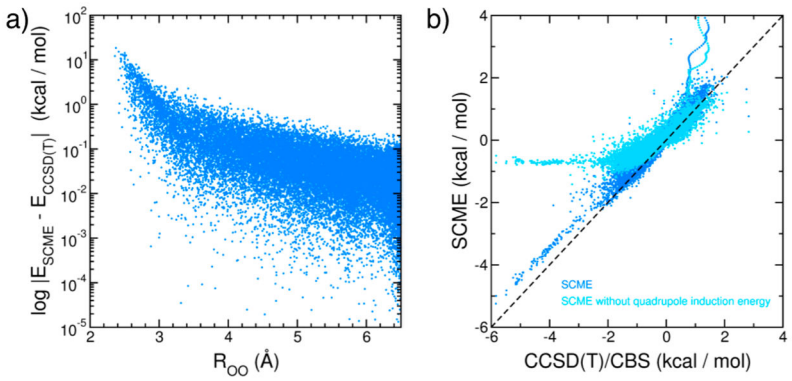

Figure 6.

(a) Logarithmic-scale errors in SCME[213] two-body absolute energies relative to CCSD(T)/CBS reference data reported in ref 191. (b) Correlation plot between SCME (*y* axis) and CCSD(T)/CBS (*x* axis) three-body energies calculated for the set of trimer geometries reported in ref 144. Results obtained with the full SCME three-body energies are shown in blue, while the results obtained when the SCME quadrupole induction energy is neglected are shown in light blue.

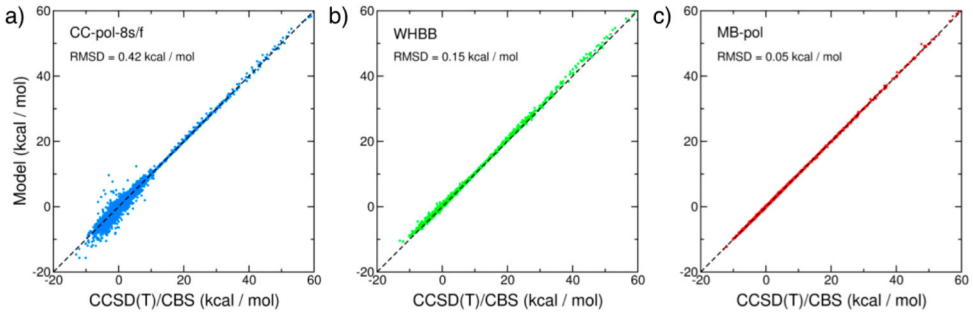

Figure 7.

Correlation plots for 2B interaction energies calculated with the CC-pol-8s/f (panel a), WHBB (panel b), and MB-pol (panel c) many-body potential energy functions. Plotted on the *x* axes are the CCSD(T)/CBS reference energies calculated for 42394 water dimers in ref 191. On the *y* axes are the corresponding energies calculated with the different water PESs.

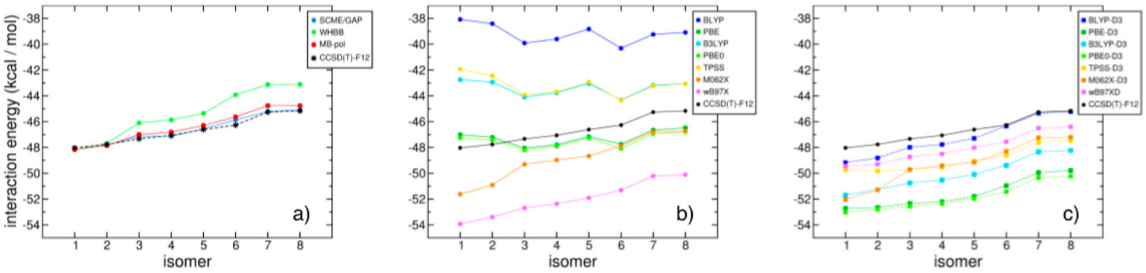

Figure 8.

(a) Interaction energies of the water hexamer isomers calculated with the SCME/GAP, WHBB, and MP-pol many-body potential energy functions using the MP2 optimized geometries of ref 218. Also shown as a reference are the corresponding values obtained at the CCSD(T)-F12 level in the complete basis set limit.[217] (b) Same comparison as in (a) using seven popular DFT models. (c) Same comparison as in (a) using the same seven DFT models as in (b) with the D3 pairwise additive dispersion correction of ref 257.

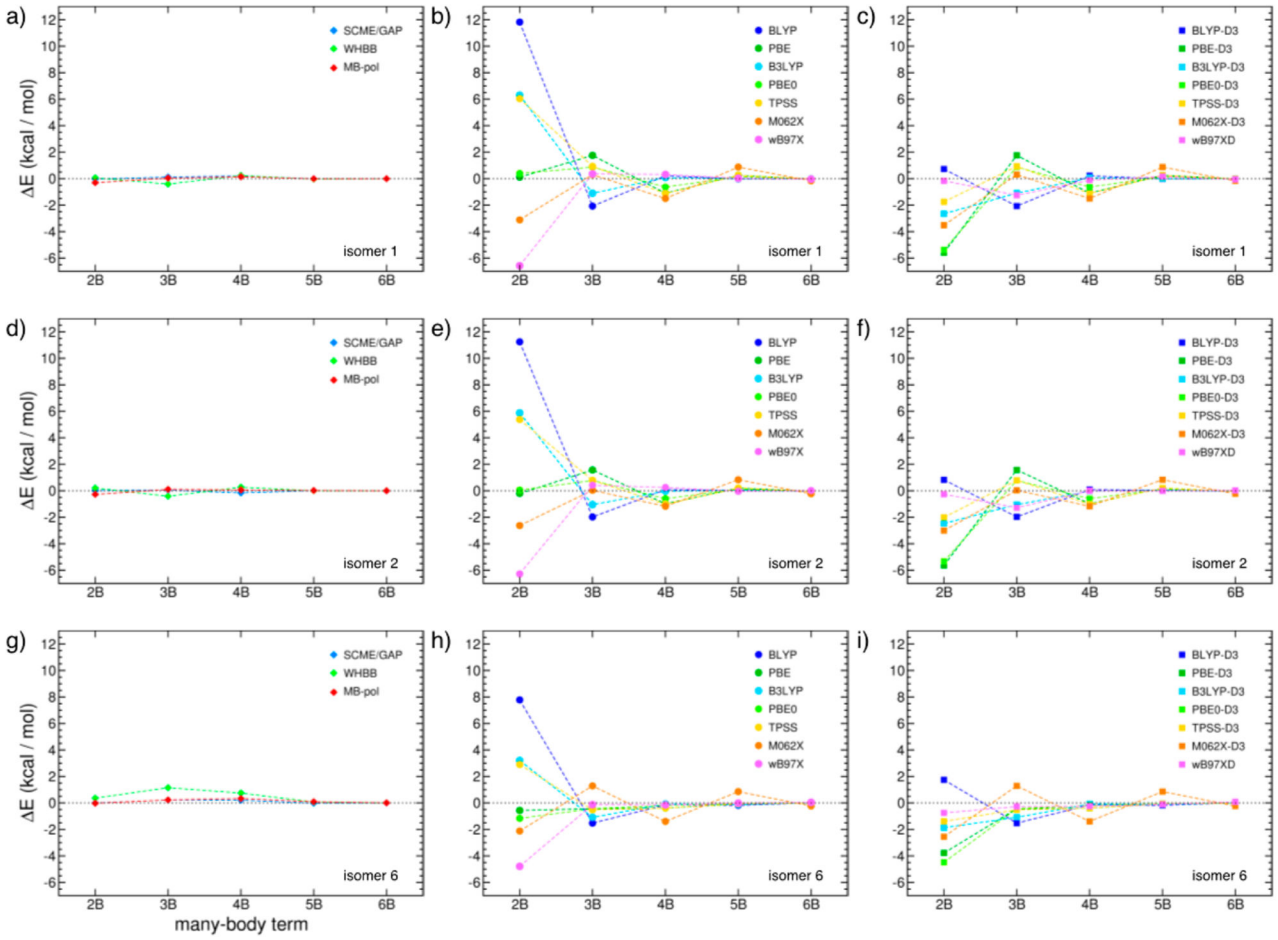

Figure 9.

Errors, $\Delta E = E_{n\mathrm{B}}^{\mathrm{model}} - E_{n\mathrm{B}}^{\mathrm{CCSD(T)}}$, relative to the CCSD(T)-F12 reference values of ref 217 for the individual terms (*n*B) of the many-body expansion of the interaction energy calculated using many-body PESs and DFT models for the (a–c) prism, (d–f) cage, and (g–i) cyclic chair hexamer isomers. The first column (a, d, and g) reports the results obtained with the SCME/GAP, WHBB, and MB-pol many-body potentials. The second (b, e, and h) and third (c, f, and i) columns report the results obtained with the same seven DFT models of Figure 8 without and with the D3 dispersion correction, respectively.

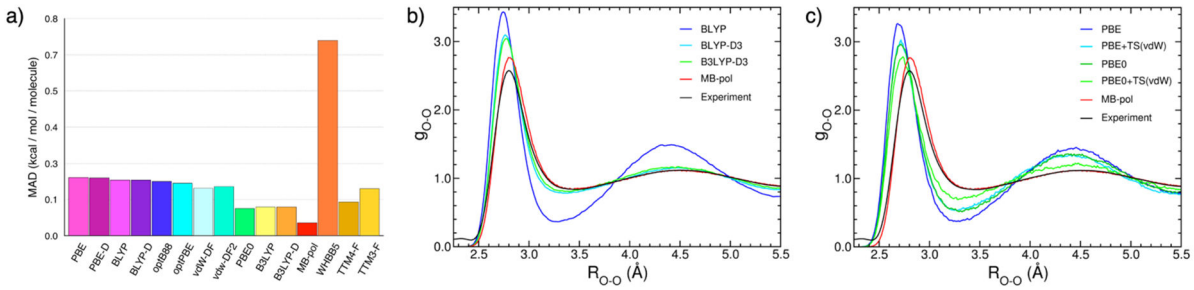

Figure 10.

(a) Mean absolute deviations in the total energy relative to quantum Monte Carlo reference data calculated using the WHBB and MB-pol many-body PESs, the TTM3-F and TTM4-F polarizable force fields, and several DFT models for configurations (in periodic boundary conditions) extracted from path-integral molecular dynamics simulations of water performed with the vdW-DF and vdW-DF2 functionals in ref 251. All data from ref 217. (b) Comparison between the oxygen–oxygen radial distribution functions calculated for liquid water in refs 249 and 292 from classical molecular dynamics simulations using the MB-pol many-body PES and the BLYP, BLYP-D3, B3LYP-D3 functionals, respectively. (c) Comparison between the oxygen–oxygen radial distribution functions calculated for liquid water in refs 249 and 293 from classical molecular dynamics simulations using the MB-pol many-body PES and the PBE, PBE+TS(vdW), PBE0, and PBE0+TS(vdW) functionals, respectively.

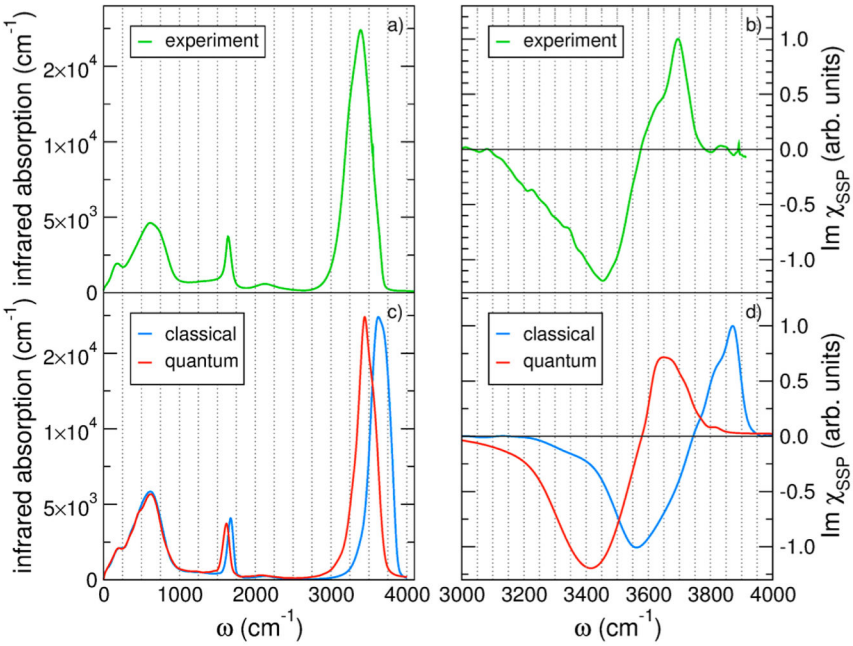

Figure 11.

Comparisons between experimental (top) and simulated (bottom) infrared spectra of liquid water (left) and heterodyne detected vibrational sum-frequency spectra of the air/water interface (right). All simulations were performed using many-body molecular dynamics (MB-MD) carried out at both classical (blue traces) and quantum (red traces) levels using the MB-pol PEF combined with many-body representations of the water dipole moment (MB) and polarizability. On the left panels, χ_{SSP} is the resonant sum-frequency susceptibility, and S, S, and P are the components related to the polarization conditions of the sum-frequency, visible, and IR beams, respectively. S and P denote beam polarizations parallel and perpendicular to the surface, respectively. See refs 261 and 90 for specific details.

Table 1

List of Polarization Models and Fitting Methodology for Various Implicit Polarizable Water Models[a]

	polarization model				data used in the fitting procedure	
model	**inducible dipole**	**inducible quadrupole**	**drude oscillator**	**electronegativity equalization**	**ab initio**	**experimental**
Stillinger and David[127]	+				+	+
polarizable electrupole[83]	+			+	+	+
Lybrand and Kollman[128]	+				+	+
Pol3[129]	+				+	+
SCP-POL[130]				+	+	+
TIP4P-POL[130]				+	+	+
T4NN[131]				+	+	
POL5[132]	+			*a*	+	
OSS[133]	+				+	
SWM4-DP(NDP)[128,129]			+		+	
SWM6[136]			+		+	+
COS[137–139]			+			+
BK3[140]			+		+	+
AMOEBA[32,135,136]	+				+	+
iAMOEBA[143]	+				+	+
AMOEBA14[294]	+				+	+
AMOEBA/GEM-DM[146]	+				+	+
Campbell and Mezey[149]	+				+	
Yoon[25]	+				+	
MCY(MCYna)[150]	+ (+)				+ (+)	
NEMO[151–157]	+				+	
X-POL[158–161]					+	
QCT[162–165]				*a*	+	
Singh-Kollman[167]	+				+	
EFP[168–172]	+				+	

	polarization model				data used in the fitting procedure	
model	**inducible dipole**	**inducible quadrupole**	**drude oscillator**	**electronegativity equalization**	**ab initio**	**experimental**
SIBFA[175–177]	+				+	
GEM*[172–174,176–178,182]	+				+	
TTM2[192–196]	+				+	
TTM3-F[40]	+				+	+
TTM4-F[41]	+				+	+
DDP2[206]	+				+	
POLIR[207]	+				+	+
POLI2VS[208]	+				+	+
ASP-W[202,203]	+	+			+	
VRT(ASP-W)III[204,205]	+	+			+	+
SCME[213]	+	+			+	

[a]The polarization model relies on machine learning.

Table 2

Compendium of Structural, Energetic, and Thermodynamic Properties[a]

Model	Structure and Energetics				Thermodynamic Properties (at 298 K)								
	g(r)	dimer	clusters	ice	ρ	ΔH_{vap}	C_p	D	ε	η	κ	α	TMD
Stillinger & David[127]		+											
Polarizable Electrupole[83]	+	+	+										
Lybrand & Kollman[128]		+		+									
Pol3[129]	+	+			●	●		●					
SCP-POL[130]		+	+		●				●				
TIP4P-POL[130]		+	+		●				●				
T4NN[131]	+	+			●	●	●				●	●	
POL5[132]	+	+	+		●	●		●	●				●
OSS[133]		+	+										
SWM4-DP		+	+		●	●		●	●				
SWM4-NDP[128,129]	+		+		●	●		●	●	●			●
SWM6[136]		+	+		●	●		●	●	●			●
COS[137–139]	+	+		+	●	●		●	●		●	●	●
BK3[140]	+	+	+	+	●	●	●	●	●	●	●	●	●
AMOEBA[32,135,136]	+	+	+	+	●	●	●	●	●	●	●	●	●
iAMOEBA[143]	+	+	+		●	●	●	●	●	●	●	●	●
AMOEBA14[294]	+	+	+		●	●	●	●	●		●		●

Model	Structure and Energetics				Thermodynamic Properties (at 298 K)							
	g(r)	dimer	clusters	ice	ρ	ΔH_{vap}	C_p	D	ε	η	κ	α	TMD
AMOEBA/GEM-DM[146]	+				●	●	●	●					●
Campbell & Mezey[149]		+											
Yoon[25]		+	+	+									
MCY[150]	+								●				
MCYna[150]									●				
NEMO[151–157]	+	+											
X-POL[158–161]		+	+		●	●	●	●	●		●	●	
QCT[162–165]	+	+	+		●		●	●			●	●	●
Singh-Kollman[167]		+											
EFp[168–172]	+	+	+										
SIBFA[175–177]		+	+										
GEM*[172–174,176–178,182]	+	+	+			●							
TTM2[192–196]		+	+	+									
TTM3-F[40]	+	+	+	+	●	●		●	●				
TTM4-F[41]	+	+	+	+		●		●	●				
DDP2[206]	+	+	+										
POLIR[207]	+	+	+	+	●			●					
POLI2VS[208]	+				●	●		●					
ASP-W2													
ASP-W4[202,203]		+											

Model	Structure and Energetics				Thermodynamic Properties (at 298 K)								
	g(r)	dimer	clusters	ice	ρ	ΔH_{vap}	C_p	D	ε	η	κ	α	TMD
VRT(ASP-W)III[204,205]		+	+										
SCME[213]	+	+	+	+									

[a]Calculated using different implicit polarizable water models as reported in the respective original studies. + indicates that the corresponding quantity is reported in the original references. All thermodynamic properties are given as deviations of the property with respect to reference experimental data: (green circles) <5%; (blue circles) 5%–10%; (red circles) >10%. In cases where a range of temperatures was analyzed in the original studies, the average deviation is reported. g(r) = radial distribution functions, ρ = liquid density, ΔH_{vap} = enthalpy of vaporization, C_p = heat capacity, D = diffusion coefficient, ε = dielectric constant, η = viscosity, κ = isothermal compressibility, α = thermal expansion coefficient, and TMD = temperature of maximum density.

Table 3

Measured and Calculated VRT Levels and Tunneling Splittings for the $(H_2O)_2$ Dimer[a]

		experiment	HBB2	CCpol-8s/f	MB-pol
$K_a = 0$					
OO	(2)	153.62(1.88)	148.57(1.14)	149.63(1.23)	154.31(2.41)
	(1)		145.00(3.48)	143.20(3.27)	149.44(1.97)
AT	(1)		128.91(0.74)	132.10(1.48)	129.44(0.24)
	(2)	120.19(0.74)	121.01(8.41)	117.50(8.67)	119.07(10.15)
AW	(2)	108.89(0.02)	105.78(0.03)	107.82(0.10)	108.87(0.13)
	(1)	107.93(2.95)	105.35(1.99)	109.23(3.29)	108.38(3.24)
DT	(1)		116.54(4.84)	113.35(5.91)	113.83(5.61)
	(2)	64.52(2.54)	67.18(2.03)	61.33(2.48)	61.31(2.54)
GS	(2)	11.18(0.65)	10.16(0.60)	12.75(0.61)	12.05(0.69)
	(1)	0.00(0.75)	0.00(0.68)	0.00(0.72)	0.00(0.81)
$K_a = 1$					
OO	(2)		152.50(1.12)	152.07(1.48)	156.60(2.71)
	(1)		150.52(1.04)	153.54(2.54)	152.69(4.13)
AT	(1)		142.25(4.33)	142.42(4.04)	143.68(4.87)
	(2)		136.24(5.31)	136.52(4.66)	137.04(5.95)
AW	(2)	123.56(3.41)	122.25(2.48)	123.12(3.16)	123.65(3.83)
	(1)	109.98(5.24)	108.95(4.55)	108.28(4.76)	109.65(5.89)
DT	(1)		94.25(2.66)	92.18(3.34)	91.22(3.47)
	(2)	87.75(1.11)	89.55(0.54)	86.37(1.32)	85.63(1.00)
GS	(2)	14.39(0.70)	14.00(0.64)	15.45(0.67)	15.04(0.77)
	(1)	11.66(0.54)	11.50(0.49)	12.36(0.51)	12.18(0.48)

[a]The energy levels are labeled as ground state (GS), donor torsion (DT), acceptor wag (AW), acceptor twist (AT), and intermolecular stretch (OO). The energies (in cm^{-1}) correspond to the origins $o_1(K)$ and $o_2(K)$ of the levels (1) and (2) with quantum numbers $K = 0$ and $K = 1$, respectively. The values in parentheses are the interchange tunneling splittings $i_1(K)$ and $i_2(K)$ defined in the text. The values for HBB2, which corresponds to the 2B PES of WHBB are taken from ref 295, those for CCpol-8sf from ref 296, and those for MB-pol from ref 191. The experimental values are taken from refs 297–301.

Table 4

Comparison between the Percentage Scores of MB-pol and Several DFT Models Computed Using the Scoring Scheme Introduced in ref 259[a]

model	f_{ss}^{mono} (cm^{-1})	E_b^{dim} (meV)	E_b^{ring} (meV)	$E_{sub}^{I_h}$ (meV)	$\Delta E_b^{prism-ring}$ (meV)	$\Delta E_b^{I_h-VIII}$ (meV)	R_{OO}^{dim} (Å)	$V_{eq}^{I_h}$ ($Å^3$)	V_{eq}^{VIII} ($Å^3$)	total
reference	3812–3835[b]	217.6	319	610	13	33	2.909–2.9127[b]	32	19.1	
MB-pol	3833	215.2	309.5	614	22.5	15	2.92	31.61	18.64	
	90, 100	100	100	100	100	90	90, 100	90	80	93, 96
LDA	60	0	–	0	–	10	0	–	–	14
PBE	50	100	80	80	0	0	100	70	20	56
BLYP	20	70	80	50	0	0	60	100	0	42
PBE0	80	100	90	90	0	0	90	70	40	62
revPBE-DRSLL	30	70	60	50	100	100	0	30	0	49
optPBE-DRSLL	40	100	100	50	100	100	60	90	30	74
optB88-DRSLL	60	100	90	20	100	100	50	50	100	74
rPW86-DF2	20	100	100	100	100	100	40	50	0	68
PBE-TS	50	80	60	0	100	40	90	30	50	56
PBE0-TS	80	90	80	40	100	60	90	40	70	72
BLYP-D3	20	100	90	30	100	40	70	50	90	66

[a] If not indicated otherwise, all reference values and DFT scores are taken from Table X of ref 259. Also listed as reference values (second entries) are the harmonic frequency of the monomer symmetric stretch and oxygen–oxygen distance in the water dimer calculated in ref 302. For MB-pol, the first entry corresponds to the value calculated for each property, while the second and, when available, third entries are the percentage scores relative to the corresponding reference values. The reader is referred to ref 259 for specific details about the scoring scheme and a complete discussion of the DFT results.

[b] From ref 302.

Table 5

Thermodynamic and Dynamical Properties of Liquid Water at 298 K as Predicted by Classical and Quantum Simulations with the MB-pol Potential[90,249a]

	density (g cm^{-3})	enthalpy of vaporization (kcal mol^{-1})	diffusion (Å^2 ps^{-1})	orientational relaxation time (ps)	surface tension (mN m^{-1})
experiment	0.997	10.52	0.23	2.5(2)[b]	71.73
classical	1.004(1)	10.9(2)	0.12(1)	5.3(2)	68(2)
quantum	1.001(2)	10.1(4)	0.22(3)	2.3(3)	–

[a] Both density (ρ) and enthalpy of vaporization (H_{vap}) were calculated in the constant temperature–constant pressure (NPT) ensemble, while the orientational relaxation time (τ_2) and diffusion coefficient (D) were calculated in the constant energy–constant volume (NVE) ensemble. If not indicated otherwise, all experimental data are taken from Table 2 of ref 62. The numbers in parentheses are the uncertainties in the last figure.

[b] From ref 303.

Table 6

Cost Associated with Different PEFs (with Flexible Monomers) for a Molecular Dynamics Step in a System Containing 256 Water Molecules in Periodic Boundary Conditions[a]

PEF	class	cost per MD step relative to q-TIP4P/F
q-TIP4P/F[37]	pairwise additive PEF	1×
TTM3-F[40]	implicit many-body PEF	7×
MB-pol[144,191,249]	explicit many-body PEF	47×

[a]All timings are relative to q-TIP4P/F,[37] an empirical point-charge pairwise additive PEF, and were obtained using a modified version of DL_POLY2 using a single core of a typical Intel Xeon E5-2640 based workstation.